

Institutionen för systemteknik

Department of Electrical Engineering

Examensarbete

Utilizing Look-Ahead Information to Minimize Fuel Consumption and NO_x Emissions in Heavy Duty Vehicles

Examensarbete utfört i Fordonssystem
vid Tekniska högskolan vid Linköpings universitet
av

Christoffer Florell

LiTH-ISY-EX--15/4906--SE

Linköping 2015



Linköpings universitet
TEKNISKA HÖGSKOLAN

Utilizing Look-Ahead Information to Minimize Fuel Consumption and NO_x Emissions in Heavy Duty Vehicles

Examensarbete utfört i Fordonssystem
vid Tekniska högskolan vid Linköpings universitet
av

Christoffer Florell

LiTH-ISY-EX--15/4906--SE

Handledare: **Martin Sivertsson**
ISY, Linköpings universitet
Magnus Fröberg
Scania CV

Examinator: **Christofer Sundström**
ISY, Linköpings universitet

Linköping, 21 oktober 2015

	Avdelning, Institution Division, Department	Datum Date
	Division of Vehicular Systems Department of Electrical Engineering SE-581 83 Linköping	2015-10-21

Språk Language <input type="checkbox"/> Svenska/Swedish <input checked="" type="checkbox"/> Engelska/English <input type="checkbox"/> _____	Rapporttyp Report category <input type="checkbox"/> Licentiatavhandling <input checked="" type="checkbox"/> Examensarbete <input type="checkbox"/> C-uppsats <input type="checkbox"/> D-uppsats <input type="checkbox"/> Övrig rapport <input type="checkbox"/> _____	ISBN _____ ISRN LiTH-ISY-EX--15/4906--SE Serietitel och serienummer ISSN Title of series, numbering _____
URL för elektronisk version http://urn.kb.se/resolve?urn=urn:nbn:se:liu:diva-122615		

Titel Title	Utilizing Look-Ahead Information to Minimize Fuel Consumption and NO_x Emissions in Heavy Duty Vehicles
Författare Author	Christoffer Florell

Sammanfattning Abstract
<p>Producing more fuel efficient vehicles as well as lowering emissions are of high importance among heavy duty vehicle manufactures. One functionality of lowering fuel consumption is to use a so called <i>look-ahead control strategy</i>, which uses the GPS and topography data to determine the optimal velocity profile in the future. When driving downhill in slopes, no fuel is supplied to the engine which lowers the temperature in the aftertreatment system. This results in a reduced emission reduction capability of the aftertreatment system.</p> <p>This master thesis investigates the possibilities of using preheating look-ahead control actions to heat the aftertreatment system before entering a downhill slope, with the purpose of lowering fuel consumption and NO_x emissions. A temperature model of a heavy duty aftertreatment system is produced, which is used to analyse the fuel consumption and NO_x reduction performance of a Scania truck. A Dynamic Programming algorithm is also developed with the purpose of defining an optimal control trajectory for minimizing the fuel consumption and released NO_x emissions.</p> <p>It is concluded that the Dynamic Programming optimization initiates preheating control actions with results of fuel consumption reduction as well as NO_x emissions reductions. The best case for reducing the maximum amount of fuel consumption results in 0.14% lower fuel consumption and 5.2% lower NO_x emissions.</p>

Nyckelord Keywords	Aftertreatment system, Dynamic Programming, Heavy Duty, Look-ahead control, Modelling, Optimization
------------------------------	---

Abstract

Producing more fuel efficient vehicles as well as lowering emissions are of high importance among heavy duty vehicle manufactures. One functionality of lowering fuel consumption is to use a so called *look-ahead control strategy*, which uses the GPS and topography data to determine the optimal velocity profile in the future. When driving downhill in slopes, no fuel is supplied to the engine which lowers the temperature in the aftertreatment system. This results in a reduced emission reduction capability of the aftertreatment system.

This master thesis investigates the possibilities of using preheating look-ahead control actions to heat the aftertreatment system before entering a downhill slope, with the purpose of lowering fuel consumption and NO_x emissions. A temperature model of a heavy duty aftertreatment system is produced, which is used to analyse the fuel consumption and NO_x reduction performance of a Scania truck. A Dynamic Programming algorithm is also developed with the purpose of defining an optimal control trajectory for minimizing the fuel consumption and released NO_x emissions.

It is concluded that the Dynamic Programming optimization initiates preheating control actions with results of fuel consumption reduction as well as NO_x emissions reductions. The best case for reducing the maximum amount of fuel consumption results in 0.14% lower fuel consumption and 5.2% lower NO_x emissions.

Acknowledgments

First of all, I would like to thank my supervisor Magnus Fröberg at Scania CV for all the support and knowledge you have provided me during my time at Scania, as well as giving me the opportunity to conduct my master's thesis at Scania.

I also would like to thank my supervisor Martin Sivertsson from ISY, the department of Vehicular Systems at Linköping University, for your input on the report and helping me understand the Dynamic Programming method. A special thanks to my examiner Christofer Sundström, also at ISY, for giving me the opportunity to write my thesis at Vehicular Systems, as well as being an invaluable support with the completion of this thesis.

Finally, I want to thank my family and friends for their support during my years at LiU. A special thanks to Karin for all the love and support you have given me in recent years.

*Södertälje, September 2015
Christoffer Florell*

Contents

Notation	ix
1 Introduction	1
1.1 Background and Problem Description	1
1.2 Purpose and Goal	4
1.3 Related Research	4
1.3.1 Look-Ahead Functionality	4
1.3.2 Modelling	5
1.4 Outline	6
2 Diesel Emission Fundamentals	7
2.1 Diesel Engine Emissions	7
2.2 NO_x Emission Control in the Diesel Engine	8
2.3 Aftertreatment Devices in a Scania EURO VI HDV	8
2.3.1 Diesel Oxidation Catalyst	9
2.3.2 Diesel Particulate Filter	9
2.3.3 Selective Catalytic Reduction Catalyst	9
2.4 Emission Certification	10
3 System Modelling	13
3.1 System Overview	13
3.2 Model Overview	14
3.3 Model Equations	17
3.3.1 Temperature Models	18
3.3.2 Mass Flow Models	20
3.4 Parametrization	21
3.5 Validation and Discussion	23
3.5.1 Parametrized Models	23
3.5.2 SCR Temperature Model	30
3.5.3 Mass Flow and Fuel Consumption	31
4 Dynamic Programming	33
4.1 DP model and Discretization	33

4.1.1	Temperature Model	33
4.1.2	Mass Flow Models	36
4.2	Evaluation Cycle	39
4.3	Objective Function	39
4.4	Constraints	41
4.5	DP Algorithm	43
5	Results and Discussion	45
5.1	Reference Values	45
5.2	Optimization Results	47
5.3	Switch Frequency Analysis	51
5.4	Optimal Mode Strategy with Simulink Model	51
6	Conclusions and Future Work	57
6.1	Conclusions	57
6.2	Future work	58
6.2.1	Modelling	58
6.2.2	Dynamic Programming	58
	Bibliography	59

Notation

NOTATION

Acronym	Meaning
<i>HDV</i>	Heavy duty vehicle
<i>CO</i>	Carbon monoxide
<i>CO₂</i>	Carbon dioxide
<i>HC</i>	Hydro carbons
<i>NO</i>	Nitrogen oxide
<i>NO₂</i>	Nitrogen dioxide
<i>NO_x</i>	Nitrogen oxides
<i>PM</i>	Particle matter
<i>PN</i>	Particle number
<i>DOC</i>	Diesel oxidation catalyst
<i>DPF</i>	Diesel particulate filter
<i>SCR</i>	Selective catalytic reduction
<i>WHTC</i>	World harmonized transient cycle
<i>WHSC</i>	World harmonized stationary cycle
<i>GPS</i>	Global positioning system
<i>EGR</i>	Exhaust gas recirculation
<i>DP</i>	Dynamic programming
<i>ECU</i>	Engine control unit
<i>PEMS</i>	Portable emission measurement system

1

Introduction

This chapter introduces the background information upon which the problem description is based. The purpose of this thesis is presented along with related research topics to the studied subject. The chapter also provides the outline of this thesis.

1.1 Background and Problem Description

Since the 1970s oil crisis, vehicle producers have experienced a continuously increasing demand from both costumers and governments to lower the fuel consumption of vehicles. The high fuel prices together with a desire for lower carbon dioxide (CO_2) emissions, have lead to the need for more fuel efficient vehicles. In relation with the demand of more fuel efficient vehicles, several governments worldwide have established emission standards, which limits the allowed levels of emissions that may be released from vehicles. The exhaust emissions from diesel engines that are regulated are carbon monoxide (CO), hydrocarbons (HC), nitrogen oxides (NO_x) and particle matter (PM) [1]. Table 1.1 shows required levels of four different EURO legislations when certifying a heavy duty vehicle (HDV) against a transient drive cycle (WHTC).

EURO	Year	CO [g/kWh]	HC [g/kWh]	NO _x [g/kWh]	PM [g/kWh]
III	2000	5.45	0.78	5.0	0.16
IV	2005	4.0	0.55	3.5	0.03
V	2008	4.0	0.55	2.0	0.03
VI	2014	4.0	0.16	0.46	0.01

Table 1.1: *EURO emissions standards for HDVs, transient certification [1]. The year column implies which year the emission standard was introduced.*

One method for lowering the fuel consumption in today's HDVs, is to make use of the Global Positioning System (GPS). Using the GPS together with the topography data and the predefined navigation route, the vehicle's optimal velocity trajectory is determined for the navigation scenario. The optimal velocity profile will lower the fuel consumption without significantly increasing the trip duration time. This control method is called "Look-ahead control"[3].

The aftertreatment system, localized after the engine, is the primary part of the HDV regarding the capacity to reduce the exhaust emission to regulated levels. It receives the polluted exhaust gases from the engine, which are created during the combustion of diesel fuel. For the system to be continuously efficient when the vehicle is in use, the aftertreatment system has to stay within certain temperature boundaries in order to efficiently reduce emissions. If the temperature is too low, the ability to reduce emissions are reduced. An example of where low temperatures may arise is when the vehicle is driving downwards a slope. An example of this phenomenon is displayed in figure 1.1. The first plot shows the engine load and the bottom plot illustrates the corresponding temperature in one part of the aftertreatment device. When the vehicle load goes down below zero Nm, the vehicle is rolling down a slope. The condition of the engine having below zero torque is determined as a motoring state, with the related motoring torque. Negative torque values indicates the amount of torque that the vehicle is producing for overcoming friction and pump losses to keep the engine running. Due to heat inertias in the exhaust and aftertreatment system, it can be seen that the the temperature drops are delayed in time in relation to the motoring state of the engine.

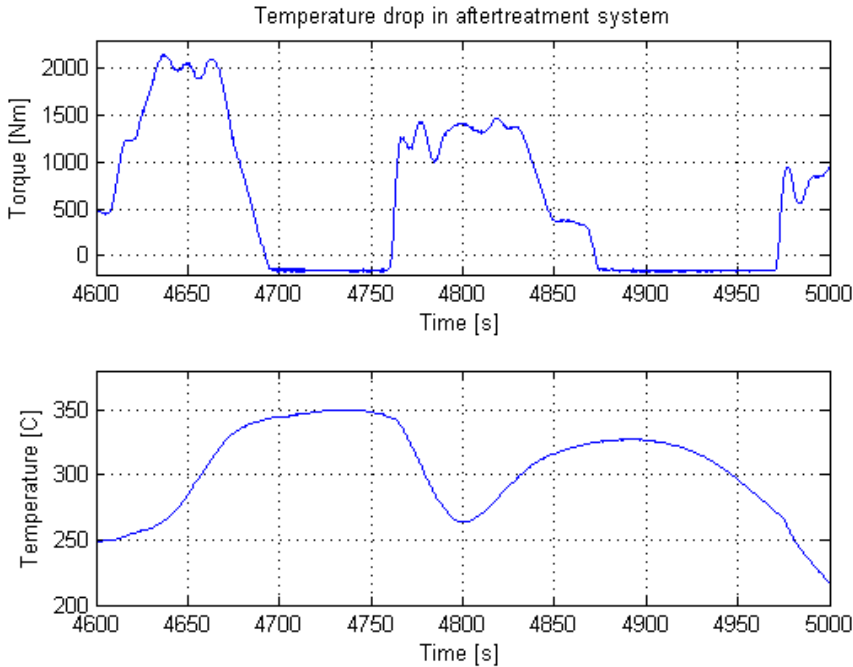


Figure 1.1: *Temperature drop in the aftertreatment system linked to the engine load condition. The measurements are recorded for a Scania HDV driving on the highway.*

To cope with the loss of performance in the aftertreatment system, the emissions from the engine must be reduced so that the emitted emissions still are within legal boundaries. The temperature must also be restored back to efficient working conditions. This is done by producing warmer exhaust gases with less emissions, through injecting more fuel into the engine than would have been required if the aftertreatment system was within its working condition boundaries.

As lowering fuel consumption is widely sought among HDV manufactures, preventing performance loss in the aftertreatment system and therefore preventing the need of injecting more fuel for heating purposes, is an interesting feature to examine. The look-ahead functionality can supply information regarding the road topography and what the optimal velocity should be in the future, the information of when the vehicle is approaching a slope is known. Based on the optimal velocity profile it is possible to model and estimate temperature losses in the aftertreatment system when the vehicle is approaching a slope. If the estimated temperatures indicate that the aftertreatment system's performance will decrease in the future, this information could be used to initiate early heating control actions. By initiating a preheating action, the aftertreatment system's temperature may still be within working conditions when the vehicle has rolled

down a slope.

1.2 Purpose and Goal

The purpose of the thesis is to investigate the potential for improvement regarding the fuel consumption, while keeping the NO_x -emissions within required levels, when utilizing a look-ahead control strategy. Other regulated emissions, mentioned in section 1.1, will not be studied in this thesis. The potential for improvement is to be examined by first creating a temperature model for the aftertreatment system in Simulink. A simplified control system, that mimics the behaviour of the control system used in a Scania HDV, is to be used with the Simulink model. The combined model and control system is to be used to illustrate today's characteristics for the aftertreatment system, in terms of aftertreatment temperatures, control signal, fuel consumption and NO_x emitted from the tail pipe.

An optimal control strategy is to be developed, using a Dynamic Programming algorithm, which will minimize fuel consumption while keeping the NO_x emissions within legal boundaries. Comparisons with the present day's performance will be made to determine if the optimization results give a desired fuel consumption and NO_x emission reduction. The calculated optimal control signal from the optimization will be used together with the Simulink model and its simplified control system, to evaluate if the optimal results are successful in regards of being a feasible preventive look-ahead control strategy.

1.3 Related Research

Related research within the thesis subject is focused on look-ahead functionality in different applications and modelling methodologies of HDV exhaust- and aftertreatment systems.

1.3.1 Look-Ahead Functionality

In the thesis by Hellström[3], the possibility to minimize fuel consumption without increasing the trip duration time, with the use of look-ahead control, is studied. Using the GPS to determine the current position and future topography in the driving path, the author formulates a predictive control problem to be solved using a Dynamic Programming algorithm. The degrees of freedom used in the calculations to minimize the fuel consumption, are vehicle velocity and gear choice. In [4] the control strategy is evaluated in a truck driving on the highway and up to 3.5% lower fuel consumption is documented.

In closer perspective of aftertreatment systems and look-ahead functionality, in the article [16] the authors investigate optimal control strategies with the use of Dynamic Programming. The purpose is to evaluate the tradeoffs in fuel economy and NO_x emission based on a lean-burn, direct injection spark ignition engine with an aftertreatment system of a three way catalyst and NO_x trap. The engine

model and aftertreatment system model is simplified to two different models using one respectively two model states. The engine parameters are expressed as an engine map based on the engine speed and engine torque. The aftertreatment system is modelled as a static three way catalyst and a dynamic NO_x trap for the one state model, and for the two state model the three way catalyst is modelled as a dynamical system.

In, [7], the authors investigate a real time fuel and NO_x controller which aims to minimize the operational costs of a diesel engine. The optimal control of system is determined through the use of Dynamic Programming, where the objective function used for minimization is based on the consumed fuel and consumed Adblue. It is shown that using a conventional Dynamic Programming algorithm produces incorrect results due to numerical calculation errors when infeasible model states are calculated in the optimization. Therefore a *Boundary-Surface Dynamic Programming* is implemented which limits the solution to always be within a feasible state space set.

In a master's thesis by Gustavsson[5], the author investigates different patent applications regarding positioning systems for look-ahead control. The author notes one possibility to control the input of urea-solution in the SCR based on future look-ahead information. At the time of the thesis publication, no patents were claimed. Gustavsson gives an example of one method of how the problem could be solved, using a vehicle model containing the dynamics of the vehicle, engine and catalyst. Using the road profile information from the look-ahead controller the optimal flow of Adblue could be calculated.

In a recent (2013) published patent application [6] the patent holders describe a method to manage the exhaust aftertreatment system using GPS, maps and traffic information. With the look-ahead data the vehicle operating condition through the travel route is predicted. The operating condition, the exhaust gas temperature profile along the travel route, is then used for controlling the aftertreatment system.

1.3.2 Modelling

Different models and modelling methodologies of exhaust system temperatures are described in [13]. The authors give examples of several different heat transfer mechanisms present in an exhaust system, and their contribution to modelling an exhaust system correctly are discussed. One static and one dynamic temperature model for calculating the temperature drop in an exhaust pipe are derived, and validation plots regarding their ability to predict temperatures are illustrated.

In the article [14], a thorough study is made to determine transient heat transfer models for determining temperatures in the exhaust system. Three models are derived with different exhaust piping configurations: a single wall of uniform pipe material and two double wall configurations with either an air gap or a specific insulation material.

In [9] a control-oriented model is derived to accurately predict temperatures from the engine and through the exhaust system and the aftertreatment components

of an HDV. The temperature models are derived from energy conservation principles inside the modelled components together with the contribution of convection and radiation to the surroundings. The chemical reactions inside the DOC, DPF and SCR are simplified to take into account the chemical energy reactions inside the components.

1.4 Outline

The thesis' outline as follows:

1. Chapter one introduces the thesis concept by explaining the background, purpose and goal as well as related theory.
2. Chapter two gives background information to diesel engine emission and technologies used for reducing emissions.
3. Chapter three describes the system studied in this thesis as well as the modelling approach and validation of the established models.
4. Chapter four presents the basic theory of Dynamic Programming and the implementation of the specific problem of this thesis.
5. Chapter five provides the optimization results with a following result discussion.
6. Chapter six provides conclusion of the thesis as well as presenting proposals for future work.

2

Diesel Emission Fundamentals

This section presents fundamental background theory of related areas to this thesis. The purpose is to give the reader basic understanding of the concepts discussed in this thesis. Fundamental diesel emission and aftertreatment concepts are described as well one example of an emission certification procedure.

2.1 Diesel Engine Emissions

The basic principle of an engine is to produce mechanical power from an air and fuel mixture. Diesel fuel is composed mainly of hydrocarbons (*HC*), with smaller amounts of other compounds, e.g. sulfur (*S*) and nitrogen (N_2), present in the fuel. During the combustion, different emissions are created which has to be treated and lowered to regulated levels. This can be done by ensuring that the engine is running close to optimal conditions and also by processing the emissions in the aftertreatment system [13].

Hydrocarbons: *HC* emissions are unburned fuel molecules which is the result of incomplete combustion of fuel. In diesel engines *HC* emissions are mainly created when a non optimal mixing condition present. This may be caused by e.g. poor mixing of air and fuel or fuel that is trapped inside the injector tip which is not exposed to the combustion flame [11].

Carbon monoxide: *CO* is created as the result of incomplete combustion reactions due to a lacking amount of oxygen or reaction temperature. Since the diesel engine is working with a lean oxygen environment, compared to the otto engine, carbon monoxide emission is generally low [11].

Nitrogen oxides: One of the dominating emissions of the diesel engine is NO_x ,

which consist of both NO and NO_2 . The creation of NO_x is situated in the layer between the fuel injection spray and flame front during combustion. Oxygen must be present in order to initiate the oxidizing reaction between N_2 and O_2 . Since the diesel engine is working in a lean oxygen environment, NO_x is easily created when the combustion temperature is sufficiently high [11].

Particulate matter: PM is the other dominating emission of a diesel engine and is the emission responsible for smoke formation from diesel vehicles. The particles consists of several different chemical compounds, e.g. carbon particles, sulphur salts, metallic oxides etc. In the general case, the different particles are classified as soot. Soot is created in local areas of the burning of fuel spray where oxygen is in lacking for optimal combustion [11].

2.2 NO_x Emission Control in the Diesel Engine

A common method to control the engine-out emissions, i.e. the emissions that is created during the combustion, is to tweak the fuel injection timings. NO_x and PM are directly related to the local temperature variations in the cylinder, particularly around the fuel injection spray. By retarding the fuel injection timing closer to the cylinder top dead center, i.e. when the piston is close to the maximum of the compression stroke, the air temperature and pressure decrease which will result in lower NO_x -emissions. However, a decreased engine-out NO_x levels does affect the PM levels in reverse with increased engine-out PM . Another downside with retarded injection time is that it is necessary to inject more fuel to achieve a stable combustion process. This is due to that the combustion cycle is not phased correctly in relation to the optimal diesel combustion cycle [10].

Another strategy to reduce the engine-out NO_x level is to fit the diesel engine with an exhaust gas recirculation system (EGR). The idea is to transfer some of the engine-out exhaust gases back to the inlet of the engine. This results in less oxygen rich environment in the cylinder which lowers the peak temperatures during the combustion process. Lower temperatures prevent the process of NO_x creation which lowers the amount of NO_x . Since less oxygen is present, the fuel vapour will not burn as efficiently as in a oxygen rich environment [13].

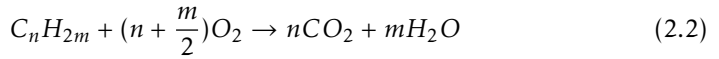
2.3 Aftertreatment Devices in a Scania EURO VI HDV

Since a couple of decades back in time, aftertreatment devices for reducing emissions have been standardized in commercial vehicles. With the increased demands on vehicles being more environment friendly, several different aftertreatment strategies have been developed, and utilized within the automotive industry. Vehicles today utilizes several components for reducing emissions. As for the aftertreatment system in Scania's HDVs the aftertreatment components are fitted inside the muffler. Three main components are used in current generation of HDVs:

1. DOC - Diesel Oxidation Catalyst
2. DPF - Diesel Particulate Filter
3. SCR-catalyst - Selective Catalytic Reduction

2.3.1 Diesel Oxidation Catalyst

The DOC is the aftertreatment system's catalytic converter for oxidizing the exhaust gases with O_2 left from the combustion process. The desired emissions to be oxidized are CO and HC to CO_2 and water [2]:



Since there are a lot of other chemical compounds present in exhaust gases from the engine the DOC may, sometimes undesirably, oxidise other products than CO , HC and PM . For this thesis, in regards to NO_x emissions one reaction is particularly worth noting, the oxidation NO to NO_2 [2]:



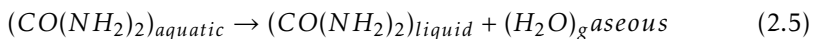
2.3.2 Diesel Particulate Filter

The DPF is where carbon based PM , commonly called soot, is removed from the exhaust gases. Particles are trapped inside the DPF and are continuously oxidised to CO_2 [2]:

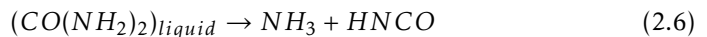


2.3.3 Selective Catalytic Reduction Catalyst

The SCR-catalyst is where NO_x is reduced to N_2 . In addition to the catalytic materials, an active reducing agent is used, called urea-solution or, by its commercial name, Adblue. Adblue is composed as a mixture of 67.5% deionized water and 32.5% Urea ($CO(NH_2)_2$). The Adblue is injected into the aftertreatment system after the DPF, and is mixed with the exhaust gases in an evaporator chamber. In order to attain a high mixing ratio with the exhaust gases, the Adblue must first be heated so that the water is evaporated[8]:



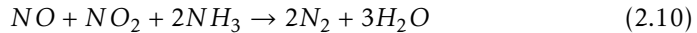
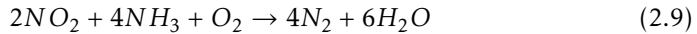
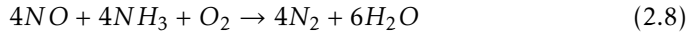
Urea is then transformed to ammonia (NH_3) and isocyanic acid ($HNCO$) by a thermolysis reaction[8]:



Lastly, HNCO is transformed to NH_3 and CO_2 through a hydrolysis reaction[8]:



The catalytic material start a chemical process between the urea-solution and NO_x that results in a mixture of CO_2 , H_2O and N_2 . The corresponding chemical reactions are:



When there is a an abundance of NH_3 , typically when the SCR temperature is low an therefore has a reduced NO_x reduction efficiency, NH_3 may slip past the SCR and react with the environment. As a safety precaution, an "ammonia slip catalyst" is installed after the SCR in order remove the overflow of NH_3 [13].

2.4 Emission Certification

In order to certify an HDV for the EURO VI legislations, the engines are tested with a number of driving cycles. A device, portable emission measurement system (PEMS), is attached to the vehicle's tail pipe in order to monitor the emissions released to the atmosphere. As previously shown in table 1.1, the emissions are measured in g/kWh. During the certification procedure the emissions are continuously measured. A simplified explanation of the method is presented below:

Every second, accumulating measurements of released emissions are started which lasts for 30 kWh of brake power, i.e. when the engine has produced a total amount of 30 kWh brake power from the beginning of measurements [15]. This is illustrated in figure 2.1 as a general example of NO_x -emissions from the tail pipe. All the accumulating measurements are usually referred as 30 kWh "windows". The accumulated amount of tail pipe emissions during a certain window is then established to a specific value of g/kWh. The bar graph in figure 2.2 illustrates an example for the specific tail pipe NO_x -values for ten different windows. Note that figures 2.1 and 2.2 are both general examples and that the data sets are not related.

The windowed values for the whole certification cycle are then evaluated against the regulated levels. For the WHTC cycle, table 1.1, a conformity factor of 1.5 is applied and multiplied to the tabulated values [15]. 90% of all the measured windowed values must pass the regulated values with the conformity factor applied. For the NO_x -emissions during a WHTC cycle the maximum value is $0.46 \times 1.5 = 0.69$ g/kWh. For the example figure 2.2, 90% of the values are saved, which means that the maximum window value in figure 2.2 is discarded. The values that are left of the saved 90% are now evaluated against the legislated value (0.69

g/kWh). The maximum value left in figure 2.2 is 0.65 g/kWh which is less than 0.69 g/kWh, which results for this example that the vehicle is approved.

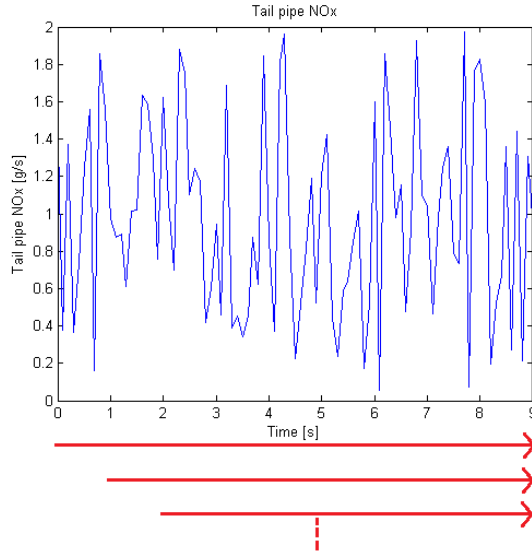


Figure 2.1: Example of tail-pipe NO_x emissions. The arrows represent the start of several measurements of NO_x emissions which are collected until the engine has produced 30 kWh of break horse power. All these measurements are saved as "measurement windows".

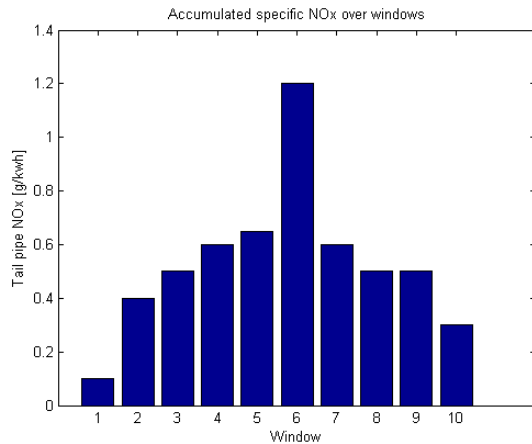


Figure 2.2: Example of window evaluation values of NO_x emissions during a ten second cycle.

3

System Modelling

This section presents an overview of the system that is studied in this thesis, together with the modelling methodology for the system. Validation plots is illustrated which will point out advantages and disadvantages with the models.

3.1 System Overview

Figure 3.1 depicts a schematic overview the system studied in this thesis.

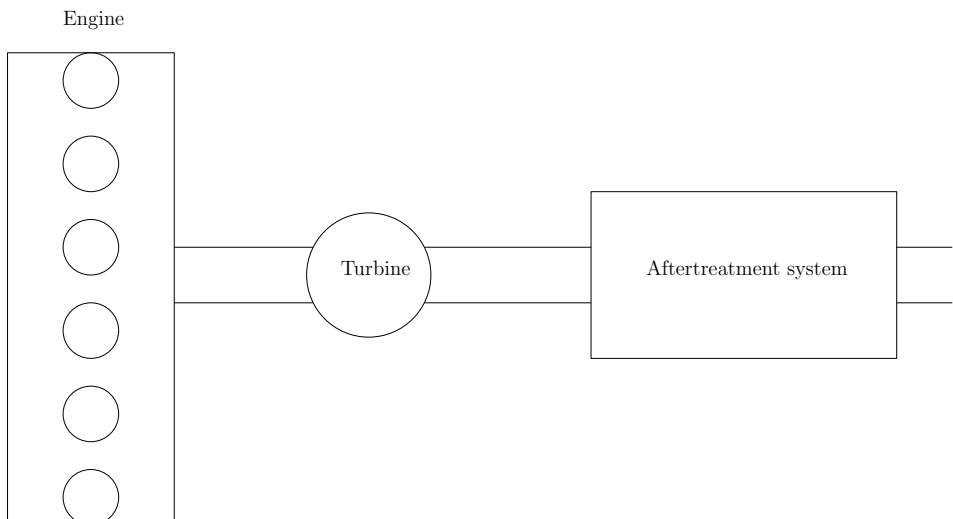


Figure 3.1: Schematic overview of the studied system.

The system consist of a 13 litre six cylinder inline engine rated at 450 horsepower. The engine is not equipped with an EGR system, all NO_x reduction is situated within the aftertreatment system. In this thesis the engine can be run in four modes which are specified by the control system for the aftertreatment system. The modes influence various engine variables, where the most significant is the fuel injection timing. Depending on which mode the engine is using, different engine-out variables are modified. The engine-out temperature, fuel consumption and engine-out NO_x emissions are particularly focused upon as significant for this thesis. These variables are influenced by the different modes according to table 3.1.

Mode	Engine-out Temperatures and Fuel Consumption	Engine-out NO_x
1	Very high	Very Low
2	High	Low
3	Medium	Medium
4	Low	High

Table 3.1: Control modes utilized in the studied system scope.

It can be seen that in order to have a high exhaust temperature for the heating of the aftertreatment system, a high amount of fuel is consumed. The engine-out NO_x is conversely related to the fuel consumption since different fuel injection timings are used between the modes. Worth pointing out is that the specifications in table 3.1 are the general results when examining the engine's specification over all working points. Local variations occur due to non-linearities in the actuators controlling the engine components.

The aftertreatment system, located after the turbine, consist of three components as explained in section 2.3. The overview of the ideal emission reduction process is depicted in figure 3.2.



Figure 3.2: Aftertreatment system overview in the studied vehicle. The chemical formulas noted above the arrows defines the emissions that are present in the exhaust flow, assuming that ideal emission reduction capability is possible. After all components, the emissions are reduced to CO_2 , H_2O or N_2 .

3.2 Model Overview

The overview of the model structure is represented in figure 3.3.

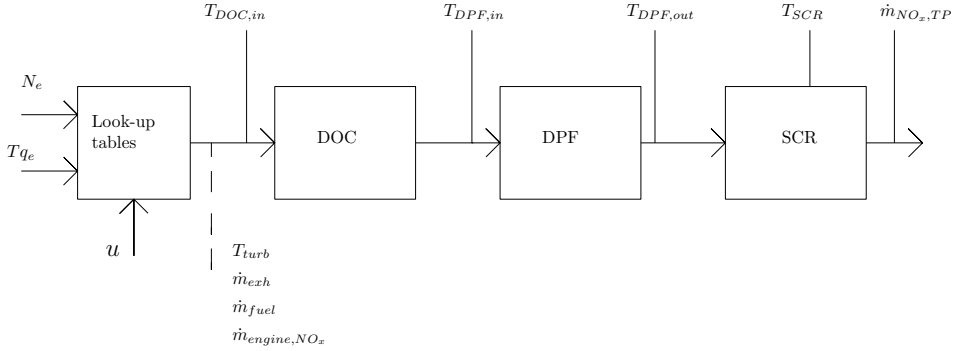


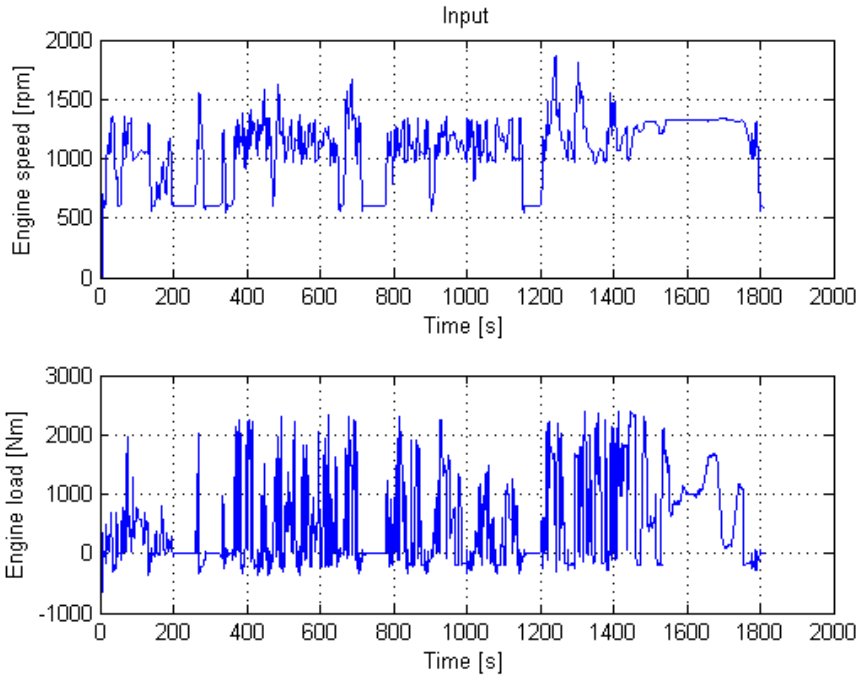
Figure 3.3: Model overview of the studied system.

The input to the model consist of engine speed N_e , engine torque T_{q_e} and the control signal u . N_e and T_{q_e} are values which are supplied from recorded cycles of the specific engine. The inputs are treated in engine specific look-up tables and outputs the four units marked with a dashed line in figure 3.3. The four outputs from the look-up tables are defined in table 3.2.

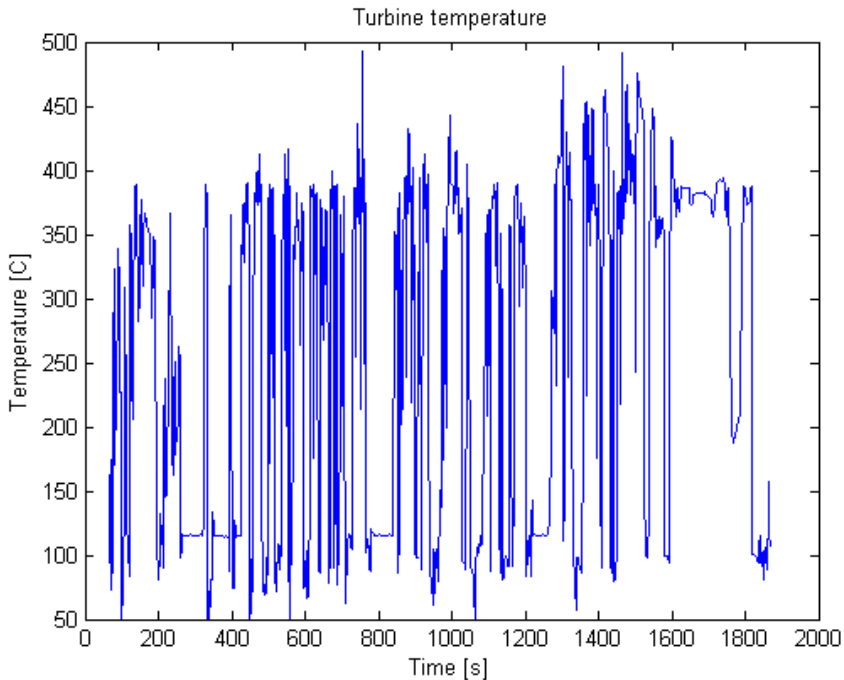
Symbol	Unit	Description
T_{turb}	K	Temperature after turbine
\dot{m}_{exh}	kg/s	Total exhaust mass flow
\dot{m}_{fuel}	kg/s	Fuel mass flow
\dot{m}_{engine,NO_x}	g/s	NO_x mass flow from engine

Table 3.2: Outputs from the look-up tables.

The look-up tables are created by running the engine in several combinations of engine speed and engine load with a constant control signal. The data is sampled when the engine has reached steady state conditions. Since there are four values of the control signal and four outputs are used, a total amount of 16 look-up tables are used. An example of the input and output from one look-up table is illustrated in figure 3.4. The input to the look-up table is shown in figure 3.4a which is based on the WHTC (World Harmonized Transient Cycle) driving cycle. The output in figure 3.4b is the turbine temperature.



(a) Input to look-up tables.



(b) Turbine-out temperature from look-up tables.

Figure 3.4: Input and example output from look-up tables during a WHTC simulation.

The measurements made for the look-up table for T_{turb} is located approximately 30 centimetres before the $T_{DOC,in}$ sensor. \dot{m}_{fuel} is measured from the fuel scale sensor and \dot{m}_{exh} is the combined mass flow of air and fuel. \dot{m}_{engine,NO_x} is established by calculating the fraction between \dot{m}_{exh} and the measurements from a NO_x -sensor located in the outlet of the engine, before the aftertreatment system.

The remaining variables for the model, which are the model outputs, are defined in table 3.3.

Symbol	Unit	Description
$T_{DOC,in}$	K	Temperature before DOC/Exhaust pipe temperature
$T_{DPF,in}$	K	Temperature before DPF/DOC-out temperature
$T_{DPF,out}$	K	Temperature after DPF
T_{SCR}	K	Temperature in SCR
$\dot{m}_{NO_x,TP}$	g/s	NO_x mass flow in tail pipe (after SCR)

Table 3.3: Output variables in the model.

3.3 Model Equations

The models to be determined can be divided into two parts, temperature models and mass flow models. Table 3.4 lists the used notation for the equations. The index i is used to indicate that several models use the same symbol with different subscripts.

Symbol	Unit	Description
\dot{Q}_i	J/s	Energy heat transfer
$c_{p,i}$	$\frac{J}{kgK}$	Specific heat
m_i	kg	Mass
\dot{m}_{exh}	kg/s	Exhaust mass flow
h_i	$\frac{J}{sm^2K}$	Convective heat transfer coefficient
k_i	$\frac{J}{sm^2K}$	Radiative heat transfer coefficient
$A_{out,i}$	m^2	Outer surface area
T_{amb}	K	Ambient temperature
I_{SCR}	kg	Heat inertia constant for SCR
η_{NO_x}	-	Maximum NO_x reduction efficiency
Δt	s	Time step

Table 3.4: The used equation symbol notation.

In this thesis the influence of the SCR-catalyst is the main topic of interest. The efficiency of the SCR will be primarily examined by its temperature, which together with the exhaust mass flow, defines the maximum NO_x conversion efficiency. The reduction of NO_x is directly related to the injected Adblue which is controlled by

the control system. The DOC and DPF are assumed to be working continuously in optimal conditions since the corresponding emissions are not of interest. The DOC and DPF will merely function as temperature models and thermodynamic restrictions in order to model the aftertreatment system accurately.

3.3.1 Temperature Models

From table 3.4, there are a total amount of four thermodynamic models, $T_{DOC,in}$, $T_{DPF,in}$, $T_{DPF,out}$ and T_{SCR} . The first three models are developed in this thesis and the model for T_{SCR} is already parametrized by Scania.

The modelling methodology used in this thesis, is based on the model formulations written in [9]. The difference in this thesis compared to [9], is that the chemical reactions inside the aftertreatment components will not be taken into consideration. The temperature changes in the different parts will solely rely on the temperature and mass flow of the exhaust gases through the components.

$T_{DOC,in}$ is modelled as an exhaust pipe where it is assumed that the temperature is uniform through the pipe. It is also assumed that the exhaust pipe behaves as a perfect heat exchanger, so that the outgoing temperature is the same as of the pipe. The internal energy change \dot{Q}_{pipe} in the pipe can be written as:

$$\dot{Q}_{pipe} = c_{p,pipe} m_{pipe} \dot{T}_{DOC,in} \quad (3.1)$$

where $c_{p,pipe}$ is the specific heat of the pipe, m_{pipe} is the mass of the pipe and $\dot{T}_{DOC,in}$ is the temperature change in the pipe. The internal energy change must be equal to the amount of energy that is transferred in and out from the pipe. Therefore \dot{Q}_{pipe} can also be written as:

$$\begin{aligned} \dot{Q}_{pipe} = c_{p,gas} \dot{m}_{exh} (T_{turb} - T_{DOC,in}) + h_{pipe} A_{out,pipe} (T_{amb} - T_{DOC,in}) \\ + k_{pipe} A_{out,pipe} (T_{amb}^4 - T_{DOC,in}^4) \end{aligned} \quad (3.2)$$

where $c_{p,gas}$ is the specific heat of the exhaust gas, \dot{m}_{exh} is the exhaust mass flow, h_{pipe} is the convective heat transfer constant between ambient air and the pipe, k_{pipe} is the radiative heat constant, $A_{out,pipe}$ is the outer surface area of the pipe. T_{amb} is the ambient temperature and is assumed to be 25 °C. The three terms between the additive signs represent the heat transferred from the inlet to the outlet of the exhaust system, the convective heat transfer with the surroundings and the radiative heat transfer. Combining (3.1) and (3.2), the temperature change in the exhaust pipe can be found as:

$$\begin{aligned} \dot{T}_{DOC,in} = \frac{c_{p,gas} \dot{m}_{exh}}{c_{p,pipe} m_{pipe}} (T_{turb} - T_{DOC,in}) + \frac{h_{pipe} A_{out,pipe}}{c_{p,pipe} m_{pipe}} (T_{amb} - T_{DOC,in}) \\ + \frac{k_{pipe} A_{out,pipe}}{c_{p,pipe} m_{pipe}} (T_{amb}^4 - T_{DOC,in}^4) \end{aligned} \quad (3.3)$$

For the following two models determining the temperatures $T_{DPF,in}$ and $T_{DPF,out}$, a similar approach is used. $T_{DPF,in}$ is assumed to be the same temperature as the outgoing temperature of the DOC since the DPF is closely attached to the DOC. Similar to the pipe, the DOC is assumed to be a perfect heat exchanger so that the outgoing temperature from the DOC is the same as the DOC temperature. With this same analogy used in equations (3.1) and (3.2) the temperature change for $T_{DPF,in}$ is determined as:

$$\begin{aligned} \dot{T}_{DPF,in} = \frac{c_{p,gas}\dot{m}_{exh}}{c_{p,DOC}m_{DOC}}(T_{DOC,in} - T_{DPF,in}) + \frac{h_{DOC}A_{out,DOC}}{c_{p,DOC}m_{DOC}}(T_{amb} - T_{DPF,in}) \\ + \frac{k_{DOC}A_{out,DOC}}{c_{p,DOC}m_{DOC}}(T_{amb}^4 - T_{DPF,in}^4) \end{aligned} \quad (3.4)$$

$\dot{T}_{DPF,in}$ is the temperature change in the DOC, $c_{p,DOC}$ is the specific heat of the DOC, m_{DOC} is the mass of the DOC, h_{DOC} is the convective heat transfer constant between ambient air and the DOC, k_{DOC} is the radiative heat transfer constant and $A_{out,DOC}$ is the outer surface area of the DOC.

The temperature change for $T_{DPF,out}$ is determined in a similar fashion as the previous models:

$$\begin{aligned} \dot{T}_{DPF,out} = \frac{c_{p,gas}\dot{m}_{exh}}{c_{p,DPF}m_{DPF}}(T_{DPF,in} - T_{DPF,out}) + \frac{h_{DPF}A_{DPF,out}}{c_{p,DPF}m_{DPF}}(T_{amb} - T_{DPF,out}) \\ + \frac{k_{DPF}A_{DPF,out}}{c_{p,DPF}m_{DPF}}(T_{amb}^4 - T_{DPF,out}^4) \end{aligned} \quad (3.5)$$

$\dot{T}_{DPF,out}$ is the temperature change in the DPF, $c_{p,DPF}$ is the specific heat of the DPF, m_{DPF} is the mass of the DPF, h_{DPF} is the convective heat transfer constant between ambient air and the DPF, k_{DPF} is the radiative heat transfer constant and $A_{DPF,out}$ is the outer surface area of the DPF.

Equations (3.3), (3.4) and (3.5) can be written in state space representation as:

$$\begin{aligned}
& \begin{bmatrix} \dot{T}_{DOC,in} \\ \dot{T}_{DPF,in} \\ \dot{T}_{DPF,out} \end{bmatrix} = \\
& \begin{bmatrix} -\kappa_{1,pipe}(T_{DOC,in}) + \kappa_{2,pipe}(T_{amb} - T_{DOC,in}) + \kappa_{3,pipe}(T_{amb}^4 - T_{DOC,in}^4) \\ \kappa_{1,DOC}(T_{DOC,in} - T_{DPF,in}) + \kappa_{2,DOC}(T_{amb} - T_{DPF,in}) + \kappa_{3,DOC}(T_{amb}^4 - T_{DPF,in}^4) \\ \kappa_{1,DPF}(T_{DPF,in} - T_{DPF,out}) + \kappa_{2,DPF}(T_{amb} - T_{DPF,out}) + \kappa_{3,DPF}(T_{amb}^4 - T_{DPF,out}^4) \end{bmatrix} \\
& + \begin{bmatrix} \kappa_{1,pipe} T_{turb} \\ 0 \\ 0 \end{bmatrix} \quad (3.6)
\end{aligned}$$

where $\kappa_{1,i} = \frac{c_{p,gas}\dot{m}_{exh}}{c_{p,i}m_i}$, $\kappa_{2,i} = \frac{h_i A_{out,i}}{c_{p,i}m_i}$ and $\kappa_{3,i} = \frac{k_i A_{out,i}}{c_{p,i}m_i}$.

In [9], h_i is determined as a three parameter model dependent on the vehicle speed. Since neither the vehicle speed is provided in the used driving cycles, nor is the vehicle speed modelled, h_i is set as a constant.

The model for the SCR temperature, provided by Scania, is modelled as a function of the exhaust mass flow and $T_{DPF,out}$:

$$\dot{T}_{SCR} = \frac{\dot{m}_{exh}(T_{DPF,out} - T_{SCR})}{I_{SCR}} \quad (3.7)$$

where I_{SCR} is a heat inertia coefficient.

3.3.2 Mass Flow Models

To determine the amount of NO_x that is released from the vehicle $\dot{m}_{NO_x,TP}$ a 2-D SCR-efficiency map, η_{NO_x} , is used. η_{NO_x} contains a percentage value of the maximum reduction capability of NO_x in the SCR. η_{NO_x} is determined as a function of T_{SCR} and \dot{m}_{exh} :

$$\eta_{NO_x} = f(T_{SCR}, \dot{m}_{exh}) \quad (3.8)$$

$\dot{m}_{NO_x,TP}$ is determined as:

$$\dot{m}_{NO_x,TP} = \eta_{NO_x} \dot{m}_{NO_x,engine} \quad (3.9)$$

For (3.9) to be valid the correct amount of Adblue must be injected in order to reduce the $\dot{m}_{NO_x,engine}$ to the $\dot{m}_{NO_x,TP}$. In the real system, the injection of Adblue is determined in a control system for the aftertreatment system. It is therefore assumed that the correct amount of Adblue is always supplied, so that (3.9) is always valid.

The mass flow of fuel, \dot{m}_{fuel} , is already provided from the engine maps. The

interesting aspect is to determine how much fuel that is consumed during the simulation of a driving cycle. The accumulation procedure to determine the consumed fuel, m_{fuel} , is expressed as

$$m_{fuel} = \int \dot{m}_{fuel} dt \quad (3.10)$$

However, as pointed out in section 3.2, the maps are of a static nature, where the \dot{m}_{fuel} is sampled at steady state points. This determines that above equation (3.10) is calculated by a quasi-static approximation. For the quasi-static calculations, the accumulated fuel in time $k+1$ is the previously accumulated fuel in k and the time specific \dot{m}_{fuel} held for the length of the time step Δt . Expressed in time step notation, i.e. discrete representation, the accumulation expression is:

$$m_{fuel}(k+1) = m_{fuel}(k) + \Delta t \dot{m}_{fuel}(k) \quad (3.11)$$

In a master thesis written by Söderstedt [12], different fuel consumption models are thoroughly researched for a 13 litre Scania engine. It is concluded that for static driving scenarios, with relatively constant vehicle speeds, the above model (3.11) will give an accurate representation of the consumed fuel. In transient driving scenarios, with varying vehicle speeds, the accuracy is reduced. The fuelling difference must therefore be examined.

3.4 Parametrization

For each of the three component models in (3.6), there are five parameters to be determined. These are:

1. h_i - Convective heat transfer constant
2. k_i - Radiative heat transfer constant
3. $A_{out,i}$ - Outer surface
4. $c_{p,i}$ - Specific heat
5. m_i - Mass

This gives a total amount of 15 parameters to be determined for all models. The six heat transfer constants, convective and radiative, are determined by a Matlab script, using the curve fitting function *fmincon* in "Matlab Optimization toolbox". The other nine parameters, surface areas, specific heats and masses, are estimated before running the curve fitting function. The estimation of these nine parameters are determined through the use of Scania's technical documentation of each component. Several iterations of the Matlab script are performed with slightly tweaked estimations of the nine predefined parameter values, as well as different datasets. The parametrization work flow of the script, as well as additional details, are as follows:

Step 1: Define dataset and engine maps.

The datasets contain both the input data to the models, N_e and Tq_e , as well as the three temperatures that the models, $T_{DOC,in}$, $T_{DPF,in}$ and $T_{DPF,out}$, are to be correlated to. Two datasets are used and acts as parameter estimation data and validation data respectively. The datasets are based on the WHTC and the WHSC driving cycles and are created in an engine test cell for the used engine. The input signals from these two cycles are seen in figure 3.4a and 3.5 respectively. The engine maps are also included, where two model variables are of interest for the parametrization, T_{Turb} and \dot{m}_{exh} :

$$T_{Turb}, \dot{m}_{exh} = f(N_e, Tq_e) \quad (3.12)$$

Step 2: Define model structure.

The model equations from (3.6) are defined. The input, output, parameters and variables are as follows:

	Input	Output	Parameters	Variables
1. $T_{DOC,in}$:	T_{Turb}	$T_{DOC,in}$	$h_{DOC,in}$	$c_{p,gas}$
	\dot{m}_{exh}		$k_{DOC,in}$	
			$A_{out,DOC,in}$	
			$c_{p,DOC,in}$	
			$m_{DOC,in}$	
	Input	Output	Parameters	Variables
2. $T_{DPF,in}$:	$T_{DOC,in}$	$T_{DPF,in}$	$h_{DPF,in}$	$c_{p,gas}$
	\dot{m}_{exh}		$k_{DPF,in}$	
			$A_{out,DPF,in}$	
			$c_{p,DPF,in}$	
			$m_{DPF,in}$	
	Input	Output	Parameters	Variables
3. $T_{DPF,out}$:	$T_{DPF,in}$	$T_{DPF,out}$	$h_{DPF,out}$	$c_{p,gas}$
	\dot{m}_{exh}		$k_{DPF,out}$	
			$A_{out,DPF,out}$	
			$c_{p,DPF,out}$	
			$m_{DPF,out}$	

Step 3: Define variables.

All models need the variable $c_{p,gas}$ and the input variable \dot{m}_{exh} . For the first model the input variable T_{Turb} is also needed. The variables T_{Turb} and \dot{m}_{exh} are defined according to (3.12) and $c_{p,gas}$ is defined in a 1-D look-up table with the input temperature to the specific model as look-up variable:

$$c_{p,gas} = f(T_i) \quad (3.13)$$

Step 4: Define parameters estimations.

Estimated parameter values for the nine parameters $A_{out,i}$, $c_{p,i}$ and m_i , are set.

Step 5: Run curve fit estimation and simulate model. Estimation of the six parameters h_i and k_i are performed. Simulations are then performed on all models with all the estimated parameters. The results from the simulations are compared against both the WHTC and WHSC cycle.

Step 6: Iterate step 4, 5 and 6. Results are saved and evaluated. The process is reiterated until a satisfactory result is achieved.

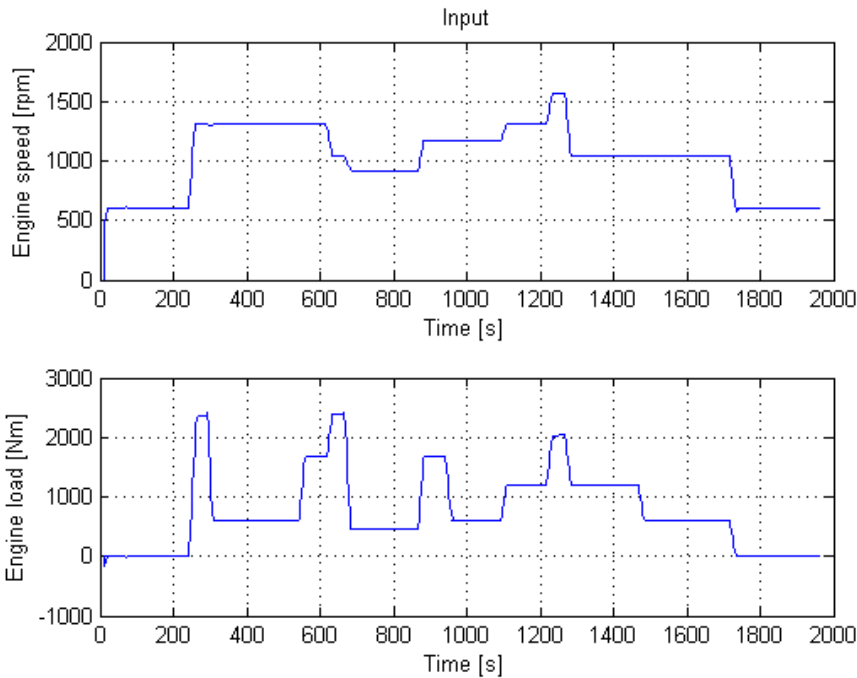


Figure 3.5: Input signals from a WHSC cycle.

3.5 Validation and Discussion

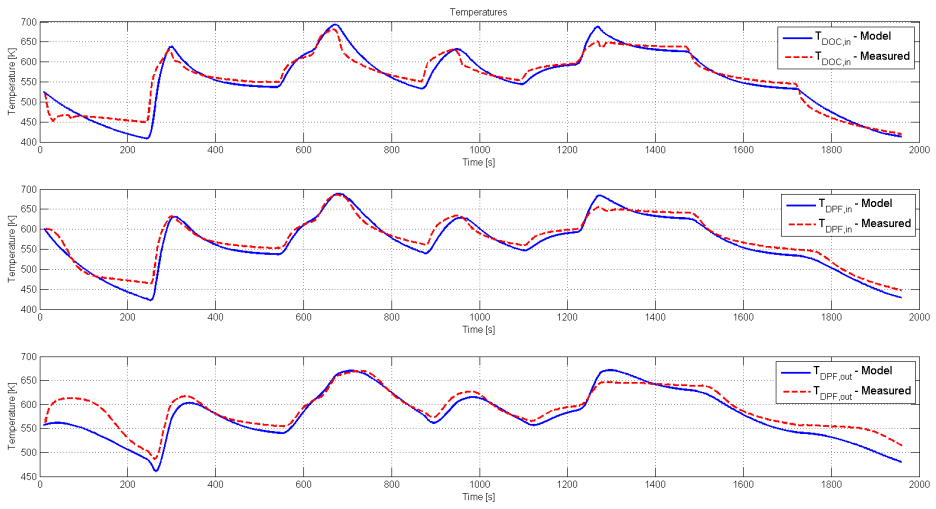
This section will illustrate plots for the various modelled aftertreatment components. The parametrization of the models have been used with both the WHTC- and WHSC cycle. The input for the WHTC cycle is previously shown in figure 3.4a and the input for the WHSC cycle is shown in figure 3.5. The mass flow model of fuel is also validated with the use of the fuel consumption model.

3.5.1 Parametrized Models

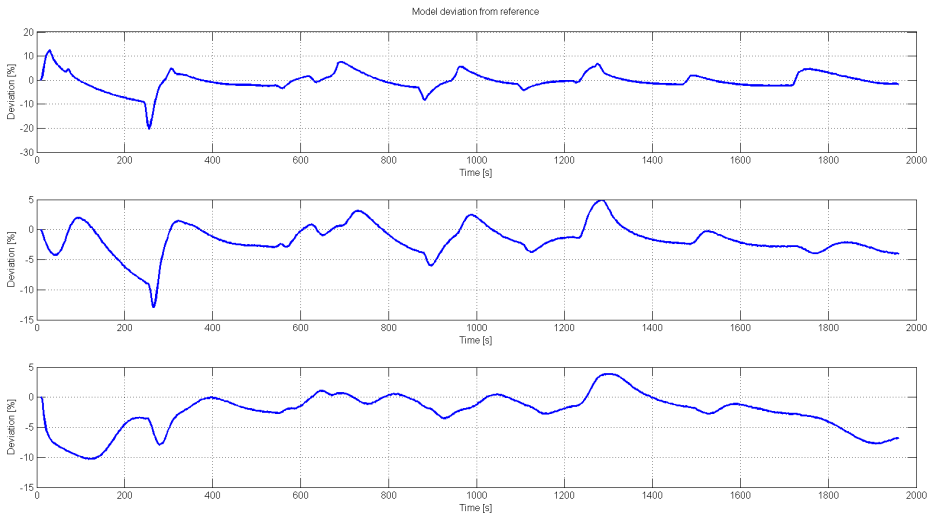
The parametrizations and validations are performed without using the simplified control system implemented in Simulink. The highest mode value (4) is chosen as constant control signal, as the reference data for both the WHSC and the WHTC

cycle uses the highest mode as constant control signal.

The complete temperature model validation with parametrized models using the WHSC cycle is shown in figure 3.6. The modelled temperature is plotted against the recorded reference temperature and is depicted in figure 3.6a. The error estimations are depicted in figure 3.6b. The corresponding results with the WHTC cycle is shown in figure 3.7.



(a) Model- and reference temperatures.



(b) Temperature error between model and reference temperature.

Figure 3.6: Temperature model validation with the WHSC cycle. The model is parametrized against the WHSC cycle.

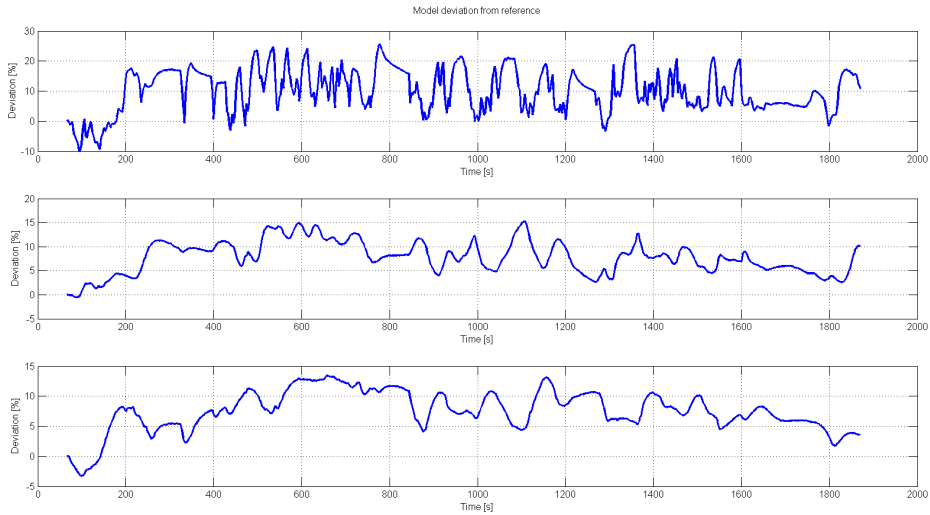
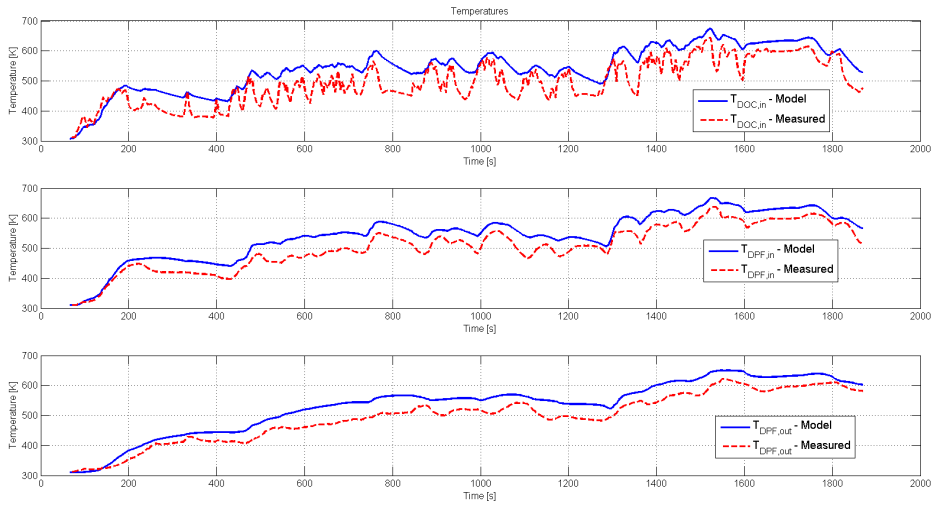


Figure 3.7: Temperature model validation with the WHTC cycle. The model is parametrized against the WHSC cycle.

The parameter k_i is determined to zero value for all three models, $T_{DOC,in}$, $T_{DPF,in}$ and $T_{DPF,out}$. h_i is given a close to zero value for $T_{DPF,in}$ and $T_{DPF,out}$. One explanation to why no outer convection or radiation are modelled for $T_{DPF,in}$ and $T_{DPF,out}$, is that the DOC and DPF are located inside the muffler. The muffler have several layers of isolation between the components and the ambient air, thus giving the components low heat transfer to the ambient air. If the terms for convection and radiative heat transfer is reduced from the presented models, the models can be written as:

$$\dot{T}_{DPF,in}, \dot{T}_{DPF,out} = \frac{c_{p,gas} \dot{m}_{exh}}{c_{p,i} m_i} (T_{i,in} - T_{i,out}) \quad (3.14)$$

This model structure can further be reduced to be written as:

$$\dot{T}_{DPF,in}, \dot{T}_{DPF,out} = \frac{\dot{m}_{exh} (T_{i,in} - T_{i,out})}{I_i} \quad (3.15)$$

which is of the same model structure as Scania's SCR model, equation (3.7).

In the results for the modelled temperatures with the WHSC cycle, figure 3.6, it is seen that that some deviations are present in the beginning of the cycle. In particular the reference data for $T_{DPF,out}$ indicates that the temperature is increasing in the beginning of the cycle, compared to what is modelled. A couple of error sources can be considered, the first being that the DPF is containing a large amount of soot in the beginning of the cycle. The temperature increase that is seen is due to that the regeneration creates heat energy and also that the blocked air flow path generates a high pressure which generates a high temperature. Another error source is that the $T_{DPF,out}$ model is deficient at modelling low load operating points, since the model also deviates from the reference temperature in the end of the cycle.

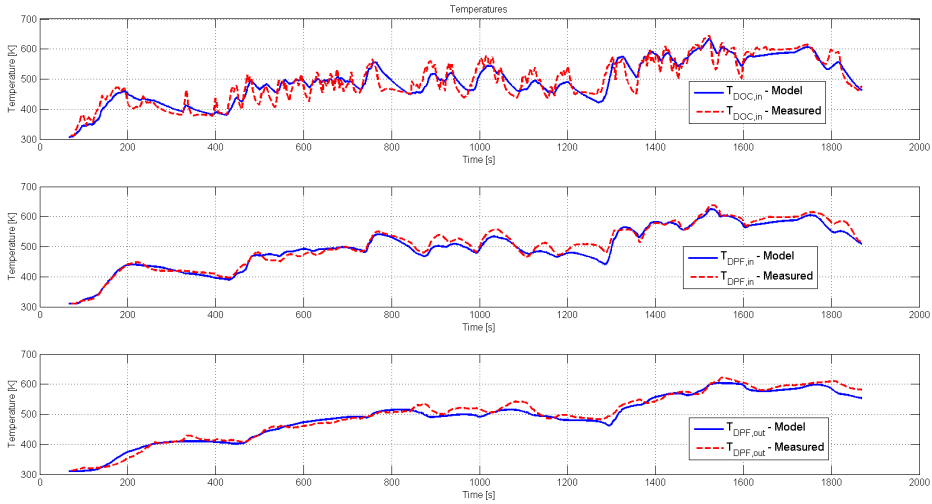
It can be seen that all temperatures are overestimated for the WHTC cycle. The main problem is the $T_{DOC,in}$ model which influence the other models with higher temperatures. The reason why $T_{DOC,in}$ is badly parametrized is explained by two factors:

The main factor is that the dynamics in a exhaust pipe is of a non-linear origin. It would be necessary to introduce several new states to the used model structure to model the system more accurately.

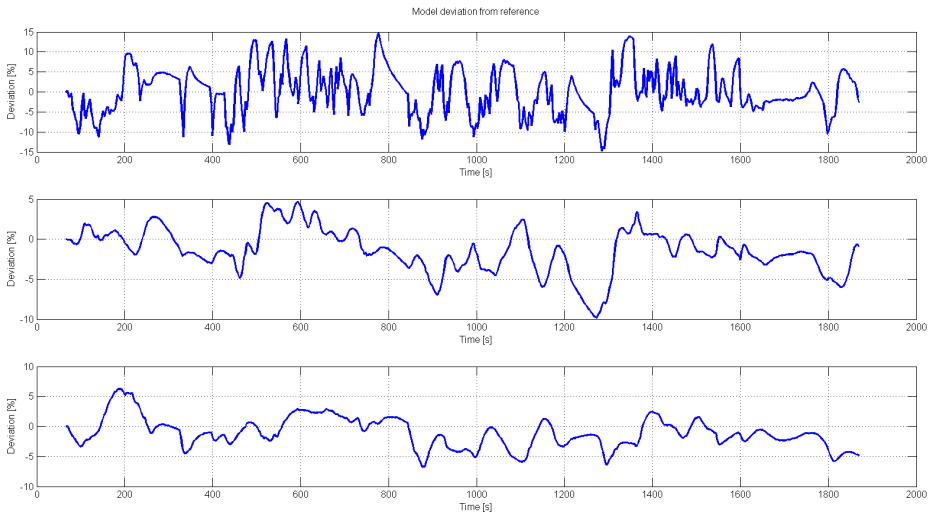
The other factor, in closer relation to the used model structure, is the simplification of the convection constant h_i . The use of a single h_i constant will make the model hard to parametrize for all types of driving scenarios. As the model is first parametrized in relation to the WHSC cycle, the fitted constant will adapt to the step response dynamics present in the WHSC-cycle. If one where to use the WHTC cycle with a more transient behaviour, the models would model transient behaviours better.

In figure 3.8 a simulation is shown during a WHTC cycle with a modified h_i value for $T_{DOC,in}$. The modified h_i value is tuned on the complete model to accurately model the temperatures on the WHTC cycle. The related result of using the modified h_i value on a WHSC simulation can be seen i figure 3.9. A better fit to the

transient WHTC cycle is now achieved, with the penalty of underestimating the temperatures in the stationary WHSC cycle.

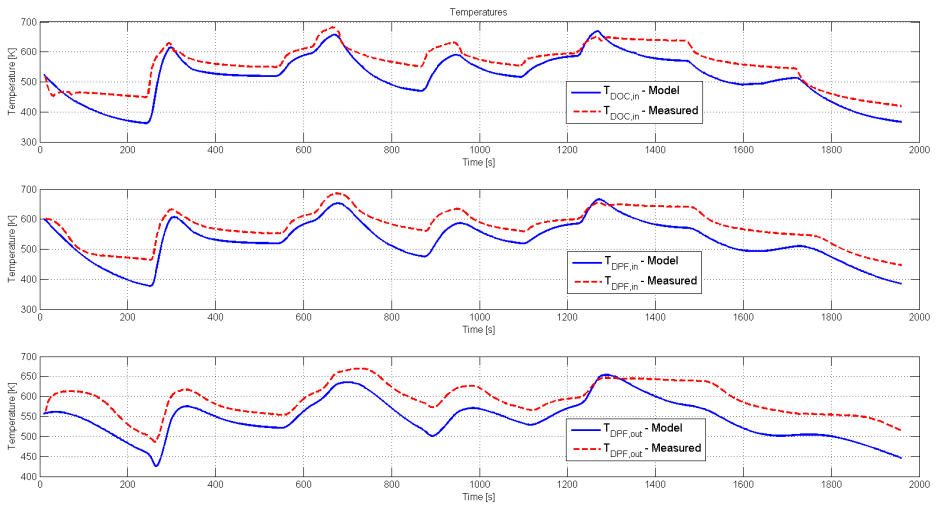


(a) Model- and reference temperatures.

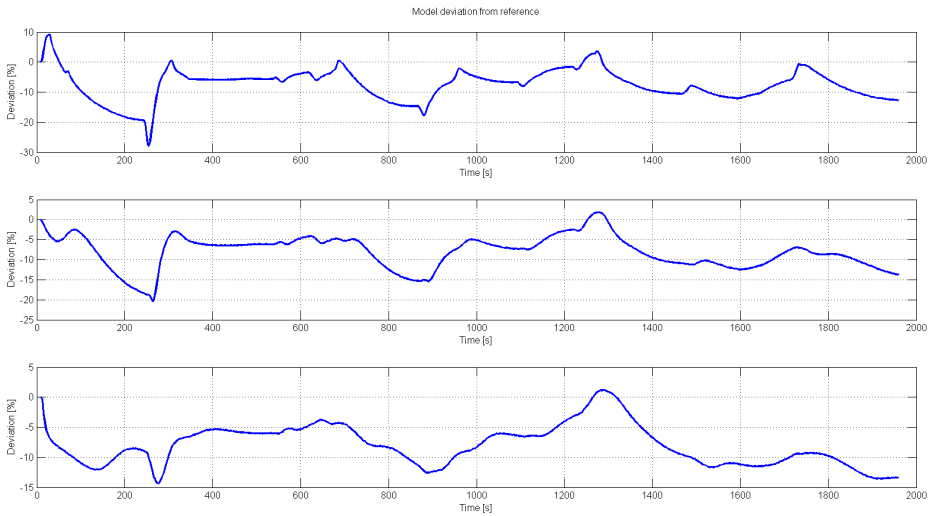


(b) Temperature error between model and reference temperature.

Figure 3.8: Temperature model validation with the WHTC cycle. The model is parametrized to achieve a better fit to the WHTC cycle.



(a) Model- and reference temperatures.



(b) Temperature error between model and reference temperature.

Figure 3.9: Temperature model validation with the WHSC cycle. The model is parametrized to achieve a better fit to the WHTC cycle.

Worth discussing is why h_i is highly dependent on what type of driving cycle that is used. h_i is supposed to explain the convection between the components and the ambient air. The previously shown figures rather indicates that it is dependent on the driving cycle's input, engine torque and engine speed. This results in the fact that the parametrization of h_i is trying to compensate for the different cycle behaviours, step response compared to transient driving. h_i should rather represent the energy transfer between the components and ambient air. Due to the low number of used parameters the model, the parametrization is not sufficient to model all types of driving cycles accurately.

The model presented in this chapter does give a relatively good model fit to validation data if the model is parametrized to a specific driving pattern. Since the transient cycle is the desired behaviour to predict accurately, the model parameters which give a better fit to the WHTC cycle is used.

3.5.2 SCR Temperature Model

The reference data for the SCR temperature is provided from the ECU, which uses the SCR model stated in (3.7). No sensor data is provided for the SCR temperature. Using the complete model from previous section, i.e. equation (3.6), and the parameters with a good fit to the WHTC cycle together with the SCR model, the results with a WHTC simulation is depicted in figure 3.10.

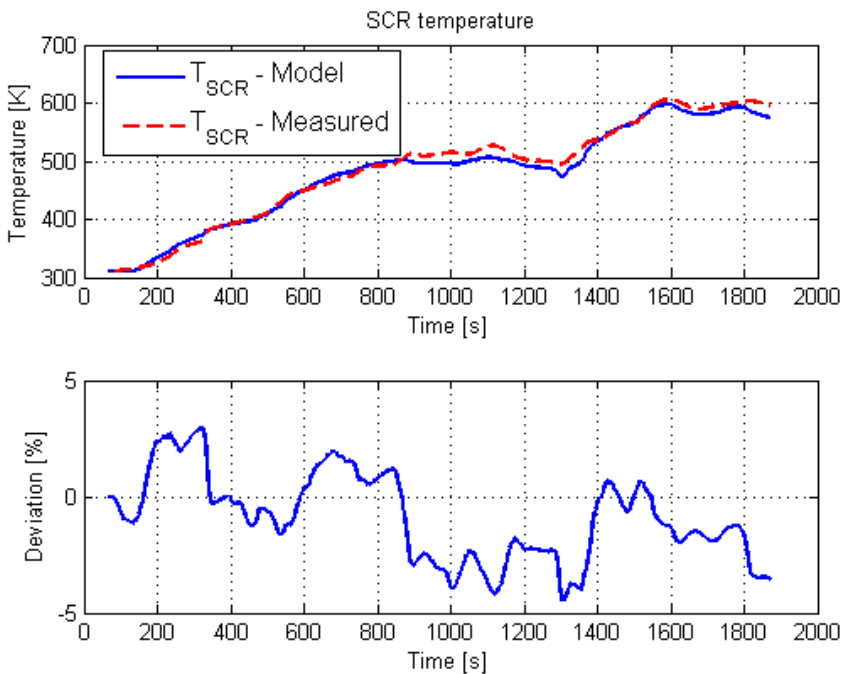


Figure 3.10: Validation of temperature model T_{SCR} .

The model does capture the temperature accurately with a maximum deviation of approximately 4.5%. The deviation from the reference is due to that $T_{DPF,out}$ is modelled slightly lower, which is seen in figure 3.8. The model for T_{SCR} is proven to be of satisfactory accuracy in regards of using the model together with a control system to establish results of the present day's performance. To establish more accurate results further work should be carried out to provide a good non-linear model of $T_{DOC,in}$.

3.5.3 Mass Flow and Fuel Consumption

To validate the fuel consumption model, equations (3.10) and (3.11), the model is compared with measurements of consumed fuel from the WHSC test cycle. The model uses a step size of 0.05 seconds. Table 3.5 presents the fuel consumption values. The model predicts approximately 3% less fuel compared the real measured value.

	Fuel consumption [g]
Model	9657
Recorded	9959
Difference	-3%

Table 3.5: Fuel consumption comparison between model and recorded values from a WHSC test cycle.

The other mass flow model, $\dot{m}_{NO_x,TP}$ is not validated in this thesis since the provided validation data does not contain this variable.

4

Dynamic Programming

This chapter presents the optimization method used for evaluating an optimal control strategy of the modes. The basics of Dynamic Programming (DP) is presented as well as the implementation steps for formulating the problem to a functional DP algorithm.

4.1 DP model and Discretization

The idea of dynamic programming (DP) is to solve complex problems by dividing the the problem into smaller subproblems. The problem is discretized in the time frame, control actions and model states in order to limit the amount of calculations needed to solve the problem. The drawbacks of dynamic programming is that it is limited to a well defined problem set. If one wants to expand the problem set, e.g. extending the number of model states, the calculation time increases exponentially [3].

4.1.1 Temperature Model

The model explained in chapter 3 uses a total amount of four temperature states to determine the SCR temperature. Using four temperature states with large discrete temperature grids for all states, will result in long computational times in a DP algorithm. As NO_x emission reduction is the chosen interest in this thesis, a direct representation of the SCR-temperature from the engine map variables is preferred. In chapter 3.3.1, the SCR temperature model is supplied by Scania as a parametrized model. This model property is of interest for the DP model. Therefore a two state model is determined by using the SCR model as well as a model for the input to the SCR model is derived. The temperature before the

SCR, i.e. temperature after the DPF, is therefore sought, $T_{DPF,out,DP}$. Figure 4.1 depicts the used DP model structure.

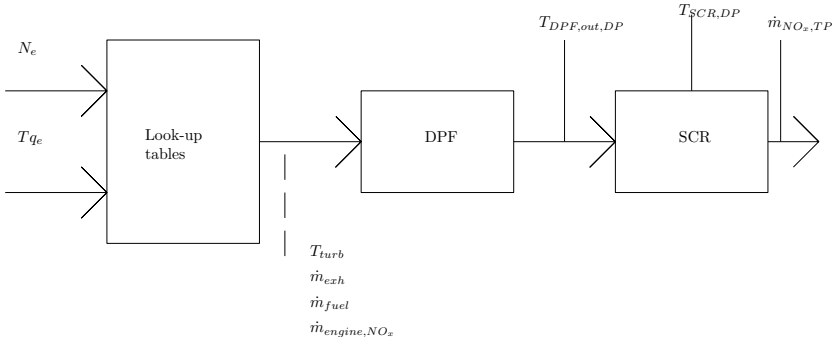


Figure 4.1: Model structure for the DP-problem. Input to the engine look-up tables are engine speed and engine load. Two temperature states are modelled, $T_{DPF,out,DP}$ and $T_{SCR,DP}$.

Using the methodology in section 3.3, equation (3.5) is modified to:

$$\begin{aligned} \dot{T}_{DPF,out,DP} = & \frac{c_{p,gas} \dot{m}_{exh}}{c_{p,DPF,DP} m_{DPF,DP}} (T_{turb} - T_{DPF,out,DP}) \\ & + \frac{h_{DPF,DP} A_{DPF,DP}}{c_{p,DPF,DP} m_{DPF,DP}} (T_{amb} - T_{DPF,out,DP}) \end{aligned} \quad (4.1)$$

where the constants $c_{p,DPF,DP}$, $m_{DPF,DP}$, $h_{DPF,DP}$ and $A_{DPF,DP}$ represents the constants to be parametrized. The difference between (4.1) and (3.5) is that the radiative constant is not included, as this constant was parametrized to zero value.

The model is discretized with the Euler forward method using a step size Δt of 1 second, resulting in the following expression for calculating $T_{DPF,out,DP}$ for the next step:

$$T_{DPF,out,DP}(k+1) = T_{DPF,out,DP}(k) + \Delta t \dot{T}_{DPF,out,DP} \quad (4.2)$$

The complete variable set to be used when parametrizing the above equation are:

	Input	Output	Parameters	Variables
	T_{Turb}	$T_{DPF,out,DP}$	$h_{DPF,DP}$	$c_{p,gas}$
$T_{DOC,in}$:	\dot{m}_{exh}		$A_{DPF,DP}$	
			$c_{DPF,DP}$	
			$m_{DPF,DP}$	

Similar to the parametrization in section 3.4, the curve fitting function *fmincon* in "Matlab Optimization toolbox" is used to determine the four parameters.

The $T_{DPF,out,DP}$ -model is seen in comparison to reference data in figure 4.2.

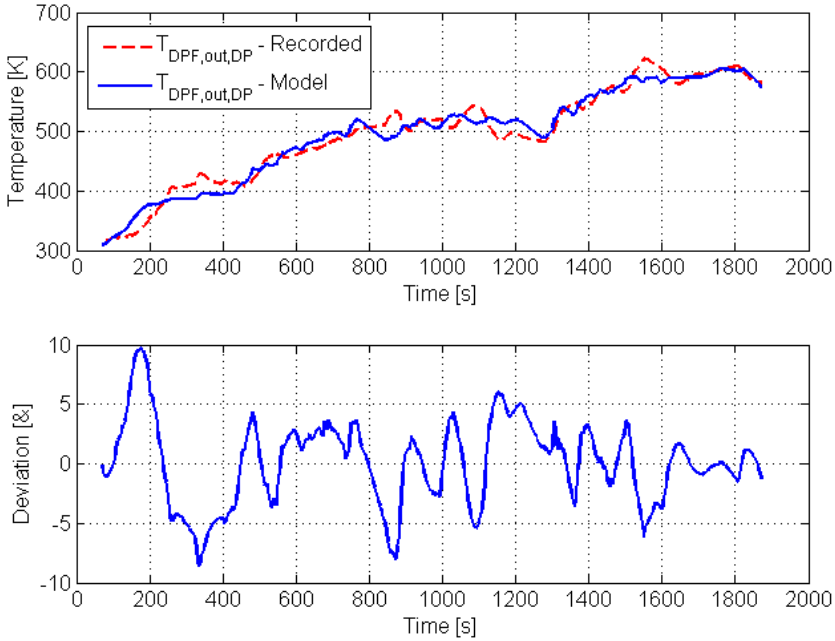


Figure 4.2: The model for $T_{DPF,out,DP}$ compared to the recorded temperature signal.

It is seen in figure 4.2 that the temperature transients are phased compared to the recorded temperature. The phasing is seen in the beginning of the cycle and at 800 seconds, where the modelled temperature increase is shifted approximately 50 seconds. The fact that a lot of dynamics between the engine and the SCR are discarded makes it sensitive to engine-out temperature and mass flow variations. On the other hand, the modelled temperature is fairly accurate to the reference, as seen in the deviation plot. The model is considered to be of sufficiently good accuracy for evaluating an optimal control strategy.

The temperature model for the SCR, (3.7), is discretized as:

$$T_{SCR,DP}(k+1) = T_{SCR,DP}(k) + \frac{\dot{m}_{exh} (T_{DPF,out,DP}(k) - T_{SCR,DP}(k))}{I_{SCR,DP}} \Delta t \quad (4.3)$$

4.1.2 Mass Flow Models

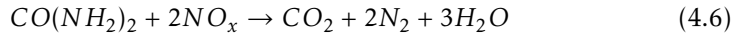
The discrete consumed fuel model is taken directly from equation (3.11):

$$m_{fuel}(k+1) = m_{fuel}(k) + \Delta t \dot{m}_{fuel}(k) \quad (4.4)$$

The mass flow of tail pipe NO_x emissions is defined from equation (3.9):

$$\dot{m}_{NO_x,TP}(k) = \eta_{NO_x}(T_{SCR}(k), \dot{m}_{exh}(k)) \dot{m}_{NO_x,engine}(k) \quad (4.5)$$

To establish a rough estimate of how much Adblue that is consumed for (4.5) a stoichiometric analysis of the chemical reactions, presented in section 2.3.3, can be made. Equations (2.5) to (2.7) states that one mole of urea molecules will create two moles of NH_3 molecules. The chemical reactions which states the NH_3 reactions with NO_x , equations (2.8), to (2.10), implies that the amount of NH_3 needed varies depending on which of the three reactions is the dominating one. It is therefore simplified that one mole of NH_3 can reduce one mole of NO_x , since this assumption states that there will always be enough NH_3 for a complete NO_x reduction. This simplification results in that one mole of urea reduces two moles of NO_x :



To calculate the amount of urea, expressed in mass per time unit ($[t.u]$), the molar mass of NO_x is assumed to be the molar mass of NO_2 ($M_{NO_2} \approx 46.0$ g/mole) is used. The mass flow of NO_x coming out from the engine (\dot{m}_{engine,NO_x}) is first calculated to moles (n_{NO_x}) per time unit and then divided by two in order to establish urea moles (n_{urea}) per time unit:

$$\frac{n_{urea}}{[t.u]} = \frac{\dot{m}_{engine,NO_x}}{M_{NO_2}} \frac{1}{2} \quad (4.7)$$

The mass flow of urea (\dot{m}_{urea}) is then calculated by multiplying $\frac{n_{urea}}{[t.u]}$ with the molar mass of urea ($M_{urea} \approx 60.0$ g/mole):

$$\dot{m}_{urea} = \frac{n_{urea}}{[t.u]} M_{urea} \quad (4.8)$$

Finally, the mass flow of Adblue is calculated by dividing \dot{m}_{urea} with the percentage of urea in Adblue:

$$\dot{m}_{Adblue} = \frac{\dot{m}_{urea}}{0.325} \quad (4.9)$$

If the above equations, (4.7), (4.8) and (4.9), are put together with the molar quantities presented in the text, it can be determined that the mass flow of Adblue is

approximately two times the amount of engine-out NO_x :

$$\dot{m}_{Adblue} = \frac{\dot{m}_{engine,NOx}}{M_{NO_2}} \frac{1}{2} M_{urea} \approx 2\dot{m}_{engine,NOx} \quad (4.10)$$

Lastly, in order to not overdose Adblue due to lacking NO_x conversion efficiency, η_{NO_x} is included to the equation:

$$\dot{m}_{Adblue}(k) \approx 2\eta_{NO_x}(k)\dot{m}_{engine,NOx}(k) \quad (4.11)$$

Since the mass flow equations, (4.4), (4.5) and (4.11) are of quasi-static nature due to the use of static engine maps, the relatively large time step of one second will produce less accurate results compared to if a smaller time step would be used. The consumption difference between using a step size of one second and a smaller step size is determined by a comparison study with the DP model, (4.4), and the Simulink model, (3.11). The two models are of the same structure, which implies that the calculated consumption difference will only be determined by the time step. The comparison was performed through simulating the DP model and Simulink model with a WHTC cycle with constant control signal. The Simulink model utilize a time step of 0.05 seconds and the DP model utilize a time step of 1 second. Figure 4.3 illustrates the accumulated fuel for both models with the use of constant mode value 1.

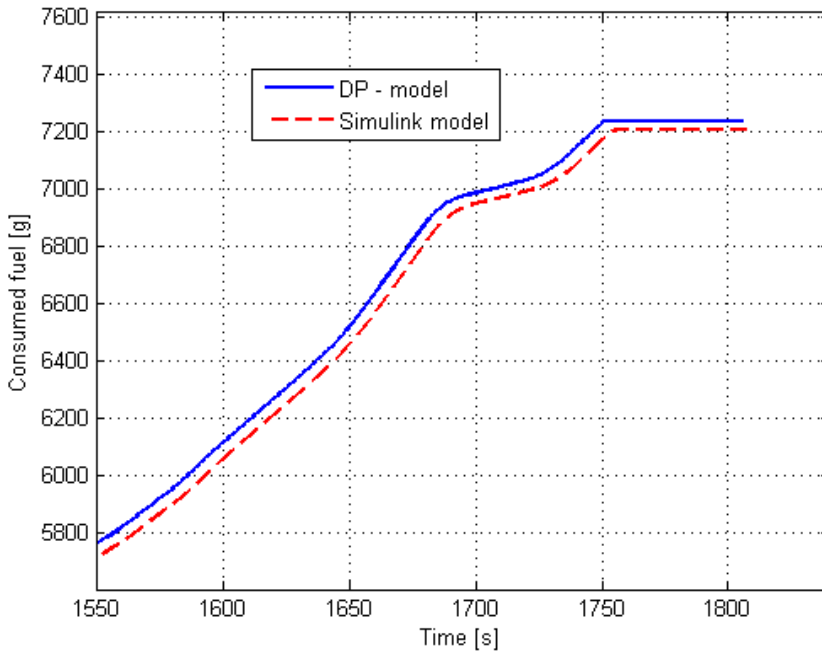


Figure 4.3: A fuel consumption comparison between the DP-model and the Simulink model. Both models utilizes the same formula, as seen in (4.4) and (3.11). The difference is that the models utilize a time step of 1 second and 0.05 seconds respectively. The simulations are performed with a WHTC cycle.

It can be seen that using a larger step size slightly increases the calculated consumed fuel. In table 4.1 the values for the different modes are shown. An average of 0.4% fuel consumption is estimated when using a larger time step, which is shown in table 4.1.

Mode	DP - Fuel consumption [g]	Simulink - Fuel consumption [g]
1	7237	7207
2	7143	7116
3	6956	6926
4	6895	6869
Average difference		0.4%

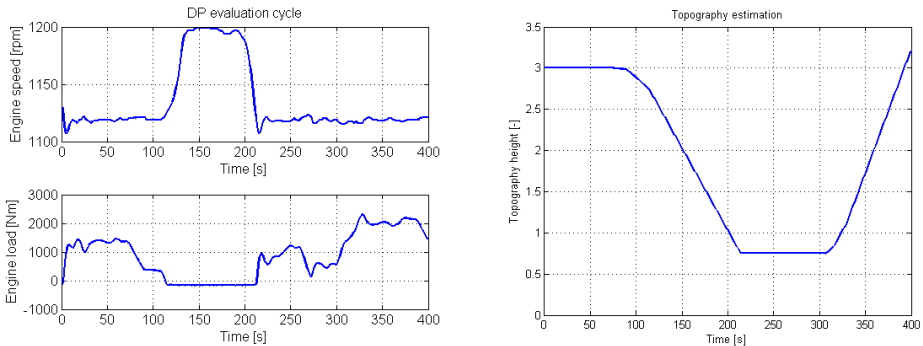
Table 4.1: The fuel consumption difference between using the DP model and the Simulink model.

A similar test was performed to determine the difference in Adblue and NO_x

emission mass flow. The four different modes are locked and for the test with NO_x emissions the conversion efficiency of NO_x was set to zero, i.e all NO_x produced from the engine were accumulated. For the test with Adblue, the simplified relation that leads to equation (4.10) is implemented to Simulink. The difference was concluded to be of the same size, 0.4%, for both Adblue and NO_x emission mass flow.

4.2 Evaluation Cycle

As pointed out in section 1.1, problems with low temperature in the SCR will occur when the vehicle is rolling down a hill, when the engine produces both low exhaust temperature and low exhaust mass flow. When the vehicle accelerates again after the downhill slope, the NO_x emissions may peak if the temperatures are too low. To minimize optimization time during the development of the DP algorithm, a small portion of a drive cycle was created. This driving scenario was established from a in house standard drive cycle, which is to drive from Södertälje to Norrköping. Figure 4.4a illustrates the engine load-speed characteristics for a 20 tonne Scania truck, using the same engine and gearbox configuration as in the data for WHTC and WHSC in previous sections. A rough estimation of the road profile is seen in figure 4.4b. The estimation is established through a general analysis of the engine speed and load characteristics in figure 4.4a. It is seen in figure 4.4a that the vehicle is coasting around 120 to 220 seconds.



(a) Profile for engine load and engine speed.

(b) Estimated road profile from 4.4a

Figure 4.4: Test scenario for the DP optimization problem.

4.3 Objective Function

When determining the objective function J at least two factors must be included, one for fuel and another for NO_x . The goal of the optimization is to determine the optimal control of the engine in respect to lower fuel consumption while having the NO_x -emissions within legal requirements. The fuel factor is easy to

formulate since the purpose is to have as little fuel consumed as possible.

Defining an optimizing goal for the NO_x emissions is not equally as straightforward as for the fuel. The definition of "within legal requirements" is a term which is difficult to define. One approach to be sure that the emission goals are met, would be to implement a virtual PEMS measuring device in the DP algorithm. As explained in section 2.4, the certification process for a vehicle requires detailed logging of released emissions over time, as well as accumulated break power, in order to have the emissions expressed in g/kWh. Implementing accumulating values over time would result in two new states being introduced each time step, one for the accumulated NO_x emissions and one for the accumulated power. This would result in a highly complex and memory consuming algorithm in Matlab. Implementing a PEMS measuring process in Matlab together with the DP algorithm would be a more demanding task for this thesis than is possible to manage within the given time frame.

Another approach would be to emulate the NO_x controller from Scania's control system in order to find a minimizing control strategy. However the controller is of a high complexity, with many different averaging states and time-evaluating memory functions. Similar to the virtual PEMS measurements, this task would be to demanding to accomplish within the thesis time frame.

The chosen objective function is to assign the two factors, fuel and released NO_x emission, as accumulating variables. The accumulation of the variables will force the objective function to minimize the total amount of consumed fuel as well as the released NO_x emissions. This will provide a solution of minimizing both fuel and NO_x . By comparing the optimal solution performance against the present performance, a conclusion can be made if the optimal solution is a feasible look-ahead control strategy.

The objective function is written as:

$$\min_J J = \sum_{k=0}^N \zeta_k(m_{fuel}, m_{NO_x,TP}) \quad (4.12)$$

where the cost at each time step is represented by ζ_k . m_{fuel} is the accumulated fuel and $m_{NO_x,TP}$ is the accumulated NO_x emissions, i.e. the NO_x released from the tail pipe. In more detail, ζ_k is expressed as:

$$\zeta_k = \beta m_{fuel}(k) + (1 - \beta) m_{NO_x,TP}(k) \quad (4.13)$$

β is used as a weight parameter for scaling how much the optimal solution should depend on minimizing m_{fuel} or $m_{NO_x,TP}$. Choosing a bad β -value will give results that either consumes more fuel or emits more NO_x compared to the present day's performance. The determination of a good β -value is made through testing several values in the range of 0 to 1.

The accumulation of $m_{NO_x,TP}$ is implemented to the algorithm as:

$$m_{NO_x,TP}(k+1) = m_{NO_x,TP}(k) + \Delta t \eta_{NO_x} \dot{m}_{engine,NO_x}(k) \quad (4.14)$$

4.4 Constraints

The control signal (u) can attain four values ranging from 1 to 4. The mode switch frequency Δu , i.e. how many times the control signal can change values in a given time period, is set to either one or ten seconds. The reason for using two different step sizes is based on two factors. The first factor for using a larger switch frequency of ten seconds is due to a quicker optimization procedure, which facilitates the development process. When a functional DP algorithm is developed, a smaller step size of one second is used for a more detailed result.

The time step of the system Δt is set to one second. The start constraints, $x_{1,2}(1)$, consists of the two modelled temperatures, $T_{DPF,out,DP}$ and $T_{SCR,DP}$. Since the evaluation cycle illustrates driving down a hill it is assumed that the vehicle is coming from a stationary condition. 250 °C (523 K) are used as start value for $x_{1,2}(1)$.

The end values for the states are left undetermined, since the purpose of the optimization is only to determine the best fuel- NO_x ratio. Therefore, the end conditions of the temperature states are not of interest.

The two temperature states are gridded with temperature steps of 20 K and are gridded between 60 and 400 °C. The reason for using a low temperature of 60 °C as the lowest possible temperature in the aftertreatment system, even though this is clearly of unreasonably low temperature during operating conditions, is because it provides a solution to handling the problem when the temperature states are calculated to be outside the desired temperature range:

If the lowest temperature is set to a value closer to what the minimum temperature is desired to be, around 200 °C, the optimization will evaluate the model states to be lower than this minimum grid value. When the optimization evaluates state points which are outside the state boundaries, this point is determined to be infeasible. To guarantee a feasible solution, the cost for this infeasible point is set to a high value. By setting a high cost to this point the DP algorithm will take into account that this point should be avoided. The high cost will imply that control actions must be initiated for the system to avoid achieving the low temperature in the specific time step. The high cost is interpolated in backwards time, as illustrated in figure 4.5. By using interpolation and a high cost, the optimal solution will provide control actions which will prevent the system of achieving the low temperature.

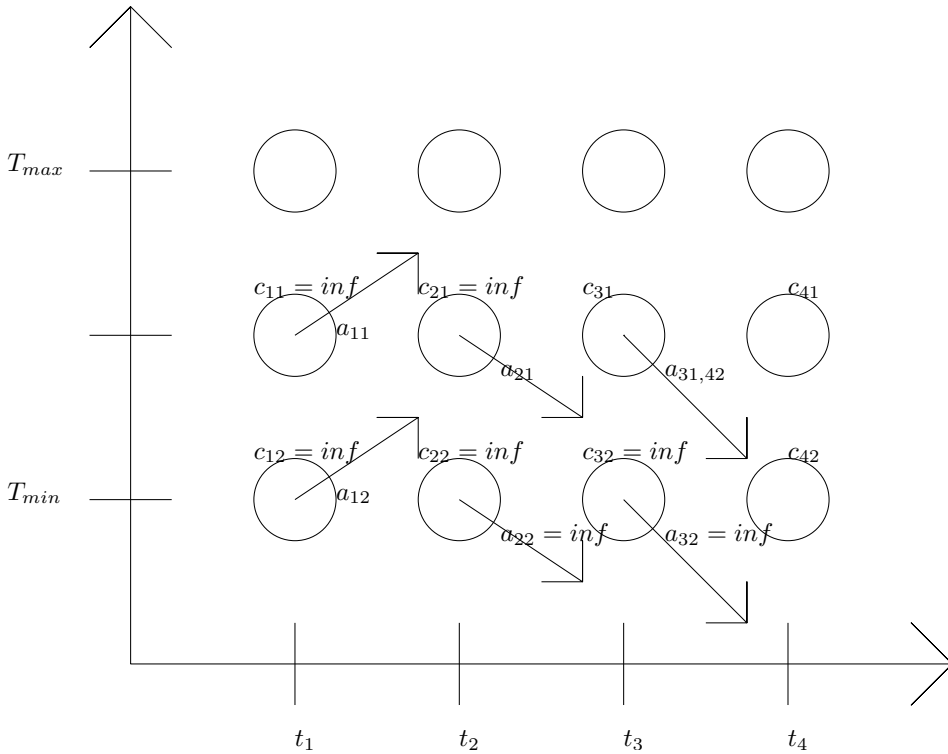


Figure 4.5: The points with costs c_{32} and c_{22} are determined to inf since the points' states are situated outside T_{min} . The points with cost c_{21} and c_{11} is determined to inf since the interpolation value between the two subsequent points will overdetermined by the large inf cost.

However, during the development process it was determined that using the interpolation strategy gave incorrect results during long coasting sections. During these sections the temperature constantly lowered since no fuel is injected, and therefore providing states that are outside the minimum 200°C . As the coasting sections were up to 100 seconds long many point were determined to high costs. One solution to the problem, according to [17], is to grid the temperature states more densely, thus providing the cost matrix with more points so that the interpolation error are not as quickly spread throughout the cost matrix. Unfortunately, it was determined that it was necessary to have small grid steps which resulted unsustainable long simulations. For the evaluation cycle of 400 seconds, the optimization took over 24 hours to complete. As many different optimization parameters are tested to compute the desired optimal control characteristics, this long simulation time was not desired.

The chosen solution is to set the lowest grid temperature to a low value. The lowest possible temperature that the model can attain is the temperature the engine provides during the coasting section. Analysing the engine maps, the lowest

temperature during coasting is slightly above 60°C. By setting the lowest state temperature to 60°C, the optimization will never evaluate state points outside the lowest grid point.

During the development of the optimization algorithm, it was also observed that the optimization results gave inconsistent optimal control signal values during coasting sections. These inconsistent results was observed as randomized switching behaviour, with no apparent reason to do so. As the engine is not supplied with any fuel during coasting, the output values from the engine maps are close to identical between the different modes. The small variations in the engine maps resulted in that the control signal was issuing unnecessary switching behaviour. To overcome this problem, a constraint was introduced which directs the system to choose the highest control mode during the coasting section. Since it is desired to minimize the consumed fuel, a control signal which uses the highest mode as much as possible during driving is considered as a wanted control signal representation. As switching modes during coasting is irrelevant for the optimal solution, the only impact this constraint will introduce is that all optimization results will depict the highest mode as the optimal control signal from 120 to 220 seconds.

4.5 DP Algorithm

The complete optimization formulation of objective function and constraints are formulated as:

$$\begin{aligned}
 \min_J \quad & J \\
 \text{Subject to} \quad & x_{1,2}(t+1) = \text{equations (4.2) and (4.3)} \\
 & x_{1,2}(0) = 523K \\
 & x_{1,2}(t) \in [x_{1,2,min}, x_{1,2,min} + x_{step} \dots x_{1,2,max}] \\
 & u(t) = [1, 2, 3, 4] \\
 & u(t_{coast}) = [4] \\
 & t = [0, \Delta t, \dots t_{end}]
 \end{aligned} \tag{4.15}$$

The optimization procedure for the DP algorithm is as follows [3]:

1. Assign final costs $J_N(x_N) = 0$.
2. Let $t = N - 1$.
3. Let $J_t(x^i) = \min_{x^j \in S_{t+1}} \left\{ \zeta_t^{i,j} + J_{t+1}(f(x_t^i, u_t^i)) \right\}$, $x^i \in S_t$.
4. Repeat 3. for $t = N - 2, N - 3, \dots, 0$.

S_t and S_{t+1} are defined as the possible states the system can achieve in time t and $t+1$. $\zeta_t^{i,j}$ is the cost to take the system from state $x^i \in S_t$ to $x^j \in S_{t+1}$. $J_{t+1}(f(x_t^i, u_t^i))$

is the cost that is calculated in the state and control signal combination at time $t+1$. Bi-linear interpolation is applied when determining $J_{t+1}(f(x_t^j, u_t^j))$, as the $f(x_t^j, u_t^j)$ may not be located at the exact grid points.

When above steps are performed J contains costs for all state and control combinations in each time step. It is now possible to find the the optimal control trajectory u^{opt} within this matrix. Given the start values of the states from (4.15), the optimal solution is determined as follows:

1. Let $t = 0$ and $x_t^{opt} = x_0$
2. Let $u_t^{opt} = \operatorname{argmin} \left\{ \zeta_t^{i,j} + J_{t+1}(f(x_t^{opt}, u_t^i)) \right\}$
3. Let $x_{t+1}^{opt} = f(x_t^{opt}, u_t^{opt})$
4. Repeat 2. and 3. for $t = 1, 2, \dots, N - 1$.

where $J_{t+1}(f(x_t^{opt}, u_t^j))$ is found by bi-linear interpolation.

5

Results and Discussion

This chapter presents the result from using the DP method on the evaluation cycle, figure 4.4a. Reference data for the evaluation cycle is first established through the use of the Simulink model together with a simplified control system. Optimization is then performed with various weight values of β to determine a result that both minimizes fuel consumption and NO_x emissions. Some of the calculated optimal control trajectories are then used together with Simulink model to evaluate the look-ahead performance in regards to consumption and emission numbers.

5.1 Reference Values

In order to make use of the DP algorithm, an estimation of what the fuel consumption and the emitted NO_x emissions are for the specific evaluation cycle is desired. With the use of the Simulink model from chapter 3, a simplified control system was developed in Simulink. The purpose of the simplified control system is to mimic the main functionality of the real control system used by Scania, in relation to the four modes that are used in this thesis. The implementation of the simplified control system was made through reading control system documentation and source code from the ECU and transferring the interesting aspects to Simulink. Calibration of the simplified control system was made through simulations in the WHTC cycle and comparing the results with recorded control system data.

The temperatures for T_{DPF} and T_{SCR} as well as the mode choice from the control system are depicted in figure 5.1 for the evaluation cycle, depicted in figure 4.4. The established consumption reference data are displayed in table 5.1.

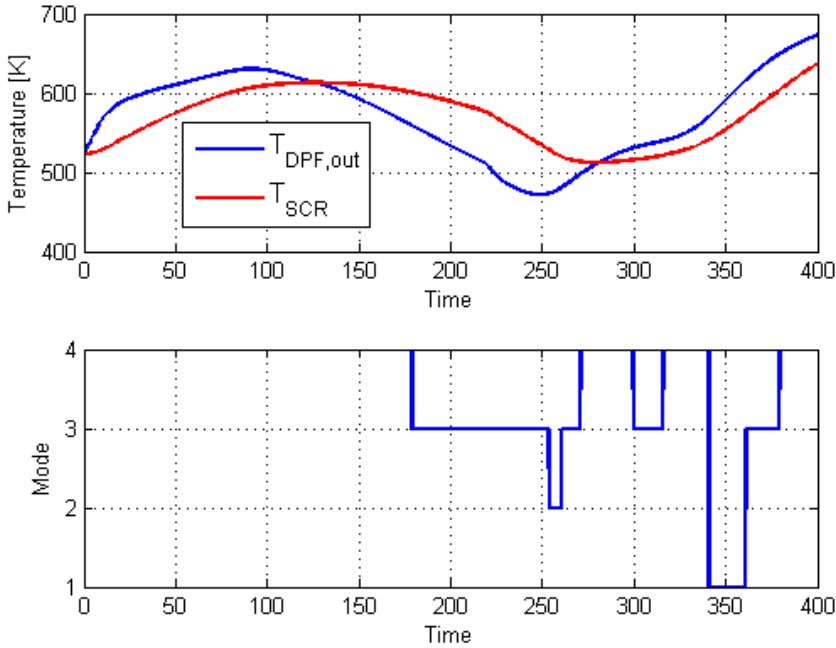


Figure 5.1: Temperatures and mode choice reference for the used evaluation cycle with the Simulink model and simplified control system.

Fuel consumption [g/kWh]	Emitted NO_x [g/kWh]	Adblue consumption [g/kWh]
198.22	0.220	21.692

Table 5.1: Reference data for fuel consumption and NO_x emissions, established from results in figure 5.1

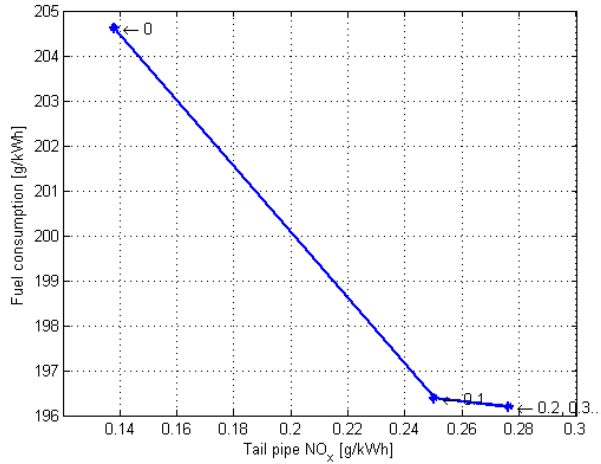
As noted in section 4.1 there is an average lower difference of 0.4% in fuel consumption, NO_x emission and Adblue consumption between the DP model and the Simulink model. To compensate for the difference, the values of this reference case is compensated by this factor:

Fuel consumption [g/kWh]	Emitted NO_x [g/kWh]	Adblue consumption [g/kWh]
199.01	0.221	21.779

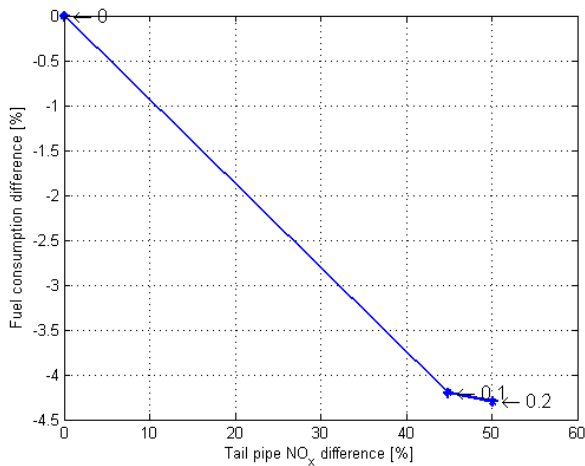
Table 5.2: Compensated reference data for fuel consumption and NO_x emissions. The values from table 5.1 are compensated with a factor of 0.4%.

5.2 Optimization Results

The optimization results, in terms of fuel consumption and accumulated Emitted NO_x , for various values of β is depicted in in figure 5.2a. The difference for the consumption numbers compared to $\beta = 0$ is depicted in figure 5.2b



(a) Optimization results.



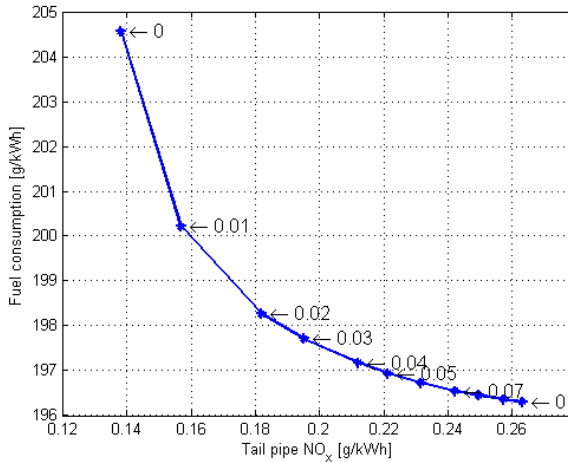
(b) Difference compared to $\beta = 0$

Figure 5.2: Fuel consumption and NO_x emissions values for various β values.

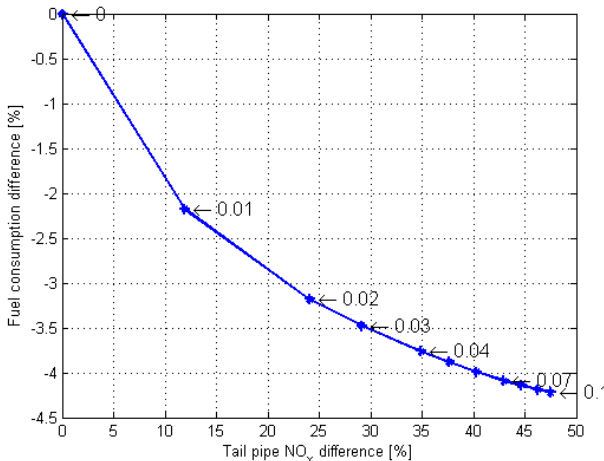
The solutions tend to have large differences in Emitted NO_x with β values from 0 and 0.1. A low β value must be chosen since the two accumulating factors of fuel

and NO_x must be scaled to be around equal value. For this cycle the NO_x factor is in the scale of two grams compared to the fuel that is in the scale around 2230 grams. This determines that the β value are to be set around values of 0 and 0.1 to scale the factors properly to acquire the desired results.

Figure 5.3 depicts a more detailed representation of β values between 0 and 0.01. Table 5.3 displays the values in more detail with the additional factor of Adblue consumption.



(a) Optimization results.



(b) Difference compared to $\beta = 0$

Figure 5.3: Fuel consumption and NO_x emissions values for various β values.

β	Fuel consumption [g/kWh]	Emitted [g/kWh]	NO_x	Adblue consumption [g/kWh]
0.00	204.58	0.138		16.92
0.01	200.21	0.157		19.55
0.02	198.26	0.182		20.82
0.03	197.71	0.195		21.42
0.04	197.16	0.212		21.91
0.05	196.93	0.221		22.20
0.06	196.72	0.231		22.35
0.07	196.53	0.242		22.47
0.08	196.44	0.249		22.60
0.09	196.35	0.257		22.64
0.10	196.29	0.263		22.72

Table 5.3: Associated fuel consumption and NO_x emissions with figure 5.3

Figure 5.4 depicts the optimization results from two β values, 0.01 and 0.04. $T_{DPF,DP}$ and $T_{SCR,DP}$ are shown in the figure along with the calculated optimal mode choice.

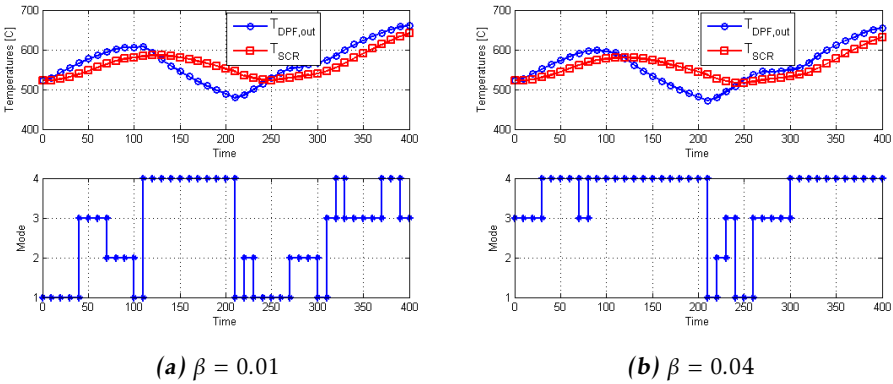


Figure 5.4: Optimization results in regards to temperature and control signal depicted for two different β values. From 110 to 210 second, mode 4 is forced to be chosen as the optimal mode for the solutions.

The use of a lower β value initiates more use of lower mode values. This is expected since a lower β implies that the objective function should focus more on lower NO_x emission. As to why both the emitted NO_x and Adblue increases with increasing β values is due to that higher mode control values are used for higher β values. A higher mode value produces more NO_x during combustion, thus is more Adblue needed in the NO_x reduction processes.

When using a mode switch frequency of one second the expected results of ad-

ditional mode switches occur, as seen in figure 5.5. The fuel consumption and emitted NO_x for β values between 0 and 0.1 are shown in table 5.4.

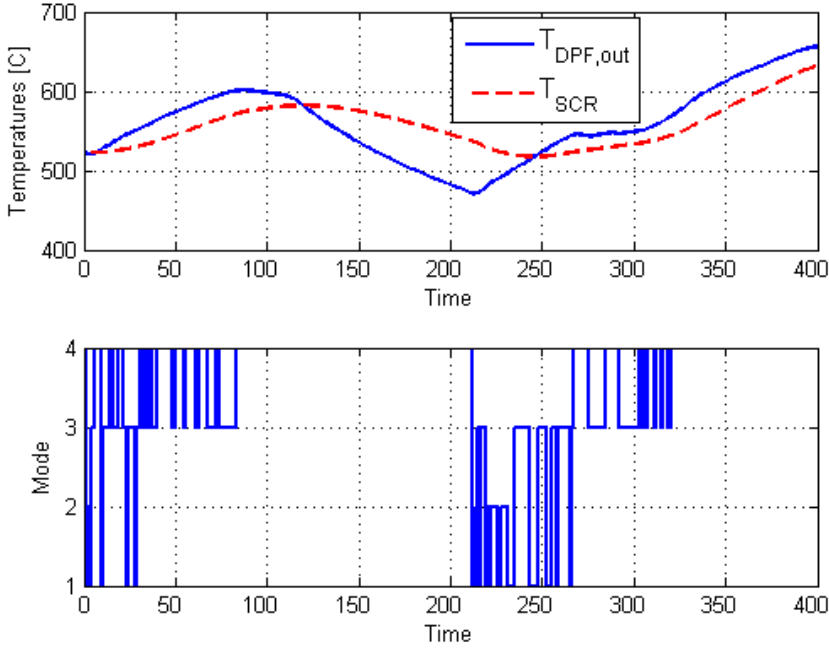


Figure 5.5: Optimization results with $\beta = 0.04$ and using a mode switch frequency of one second.

β	Fuel consumption [g/kWh]	Emitted [g/kWh]	NO_x	Adblue consumption [g/kWh]W
0.00	204.58	0.138		16.92
0.01	200.41	0.155		19.47
0.02	198.38	0.178		20.90
0.03	197.55	0.195		21.50
0.04	197.13	0.208		21.89
0.05	196.83	0.218		22.22
0.06	196.72	0.225		22.31
0.07	196.65	0.228		22.39
0.08	196.55	0.235		22.54
0.09	196.44	0.246		22.62
0.10	196.38	0.250		22.68

Table 5.4: Fuel consumption and NO_x emissions with the use of several β values and a mode switch frequency of one second.

Comparing the two solutions using different mode switch frequency and $\beta = 0.04$, it is determined that there is less than 0.02% difference in fuel consumption. The emitted NO_x difference is of a larger fraction, 1.9% lower emission in favour of using a mode switching frequency of one second.

5.3 Switch Frequency Analysis

Figure 5.6 depicts two comparison figures of the SCR temperature and NO_x emission between using one and ten second mode switch frequency with the use of $\beta = 0.04$. The SCR temperature is one to two Kelvin higher throughout the simulation beginning from around the 20th second of the simulation. This slightly higher temperature results in a higher NO_x reduction efficiency which, together with that lower modes gives lower engine-out NO_x , gives an impact on the accumulated NO_x emission throughout the cycle.

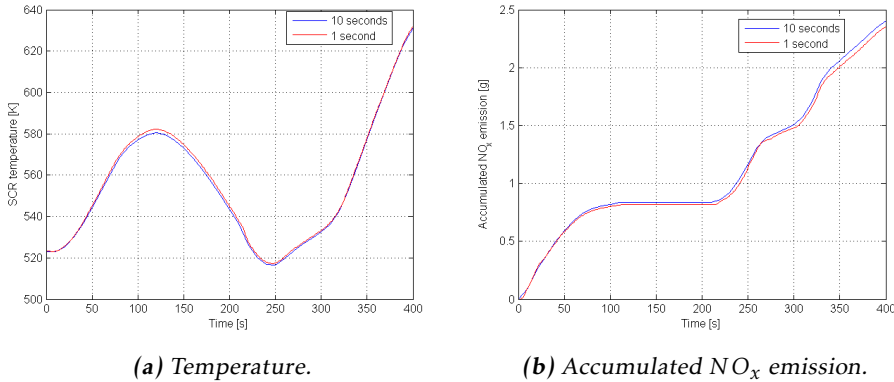


Figure 5.6: Comparison figures between using a mode switch frequency of one second and ten seconds. Results are shown with $\beta = 0.04$.

To judge the plausibility of utilizing these optimal mode choices in a vehicle, the case of a mode switching frequency of one second can be perceived as bit jumpy. Even though the control system is designed to operate at one Hz, this behaviour is not suitable. The reason the jumpy appearance is present is because that in many operating points, two modes can have close to identical fuelling rates and engine-out NO_x . As the factors are close to identical, the slightest tenth of a decimal point in favour of one mode gives a lower cost which triggers a mode switch. The case of using ten seconds is a more desired operating appearance.

5.4 Optimal Mode Strategy with Simulink Model

The calculated optimal control modes are used together with the Simulink model to find out the resulting control signal from the control system. As the Simulink

model is the factor which defines the reference values for consumed fuel and emitted NO_x , the result of using the calculated optimal mode signal on the Simulink model will prove if savings can be made.

Figure 5.7 depicts T_{DPF} and T_{SCR} when using the calculated mode signal for $\beta = 0.04$ and a mode switch signal of 10 seconds. The solid line in the second plot is the optimal mode signal and the dashed line is the resulting mode that the simplified control system outputs. Table 5.5 contains the resulting data and the uncompensated reference data from table 5.1

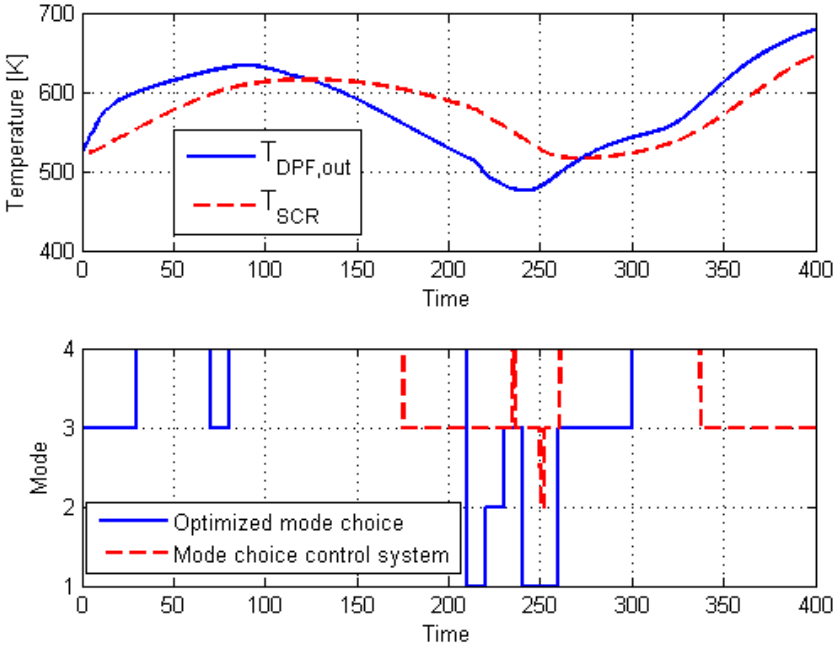


Figure 5.7: Results of using the mode signal from figure 5.4b. The solid mode signal is the calculated optimal mode choice and the dashed mode signal is the related behaviour of the control system. The solid optimal mode is the used control signal through the simulation.

	Fuel consumption [g/kWh]	Emitted [g/kWh]	NO_x	Adblue consumption [g/kWh]
Reference	198.22	0.220		21.692
$\beta = 0.04$	197.87	0.194		21.983
Difference	-0.18%	-11.6%		+1.35%

Table 5.5: Results for fuel consumption and NO_x emissions from the reference case, table 5.1, and the simulation in figure 5.7.

It can be seen that by using a slightly more aggressive approach with the use of mode 3 around 0 to 80 seconds and mode 1 around 220 to 270 seconds, results in that 0.18% fuel can be saved and 11.6% lower NO_x emissions with the compensation of using 1.35% more Adblue compared to the reference case. More Adblue is needed since mode 4 is used after 300 seconds. During this section the engine is used with a high load, as seen in figure 4.4a, which produces a lot of NO_x from the engine. As the temperature in the SCR is sufficiently high to reduce the NO_x , more Adblue is need.

These results however indicate that in the last 350 seconds the control system wants to lower the mode value to 3. This results in that the calculated mode choice for $\beta = 0.04$ cannot be considered a valid solution since the control system indicates that a lower value must be chosen. As the control system is used to define the allowed NO_x emission, the last mode switch must be included for a valid solution. This aspect is implemented to the simulink model as:

$$u = \min(u^{opt}, u_{control}) \quad (5.1)$$

where u^{opt} is the predefined calculated optimal mode trajectory and $u_{control}$ is the control system output.

Figure 5.8 depicts four simulations with the optimal mode control signal of four different β values. The calculated optimal mode value is shown as a solid line and the control systems mode value as a dashed line in the upper subplot. The resulting mode used in the calculations are shown in the lower subplot. Consumption numbers are shown in table 5.6.

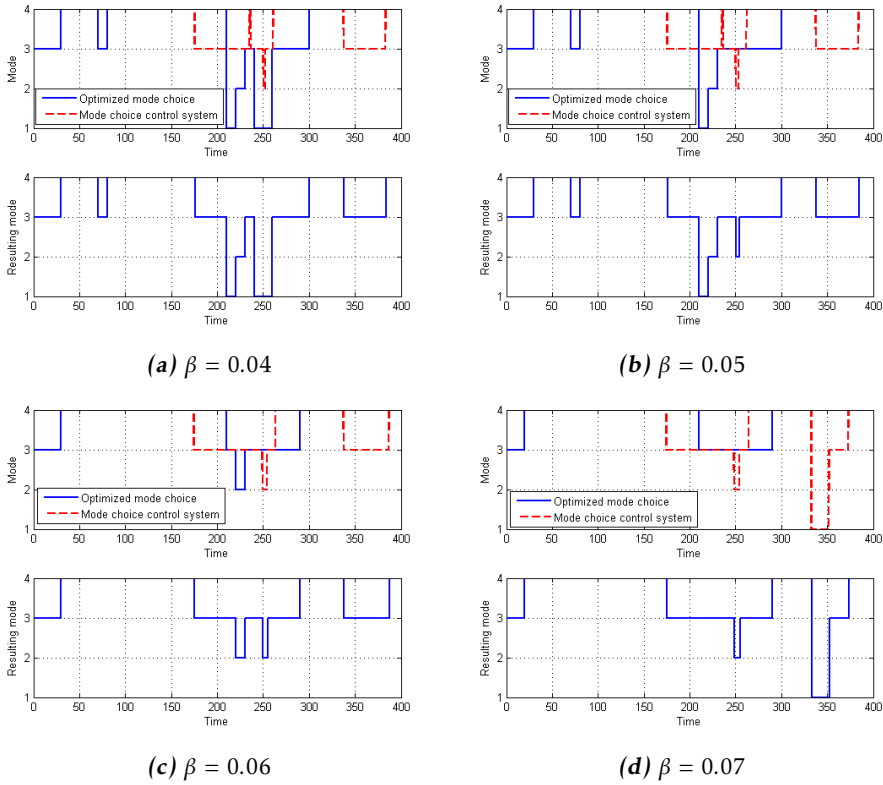


Figure 5.8: The first sub-plot depicts the calculated optimal mode choice as the solid line and the related behaviour of the control system is the dashed mode signal. In the second sub-plot is the resulting mode, i.e the minimum value of the two mode signals, that is used in the simulations are shown.

	Fuel consumption [g/kWh]	Emitted [g/kWh]	NO_x	Adblue consumption [g/kWh]
Reference	198.22	0.220		21.692
$\beta = 0.04$	198.26	0.192		21.266
Difference	+0.02%	-13.0%		-1.96%
$\beta = 0.05$	198.08	0.198		21.486
Difference	-0.07%	-9.95%		-0.94%
$\beta = 0.06$	197.95	0.209		21.562
Difference	-0.14%	-5.20%		-0.61%
$\beta = 0.07$	198.31	0.215		21.557
Difference	+0.04%	-2.45%		-0.57%

Table 5.6: Results for fuel consumption and NO_x emissions from the reference case, table 5.1, and the simulations in figure 5.8.

The results in table 5.6 shows that the $\beta = 0.04$ result in a higher amount of consumed fuel compared to the reference case. The use of $\beta = 0.06$ is concluded to be the best case scenario for reducing fuel consumption, with a lower fuel difference of 0.14% and 5.20% lower NO_x emissions. It is also seen that the turning point for a case with increased fuel consumption occurs at $\beta = 0.07$.

The result of using the optimal strategy on the Simulink model indicates that it is possible to initiate preventive control actions to lower the fuel and NO_x emissions. By utilizing a more aggressive approach, i.e. using lower mode values before high engine loads, the simulation indicate that 0.14% fuel could be saved. Assuming that one has perfect look-ahead information of the future it would be possible to initiate this aggressive control approach to compensate the future need of lowering the mode during high loads.

In chapter 1.1 an exposition was presented that it would be possible to initiate preventive preheating actions before a coasting section to have the aftertreatment system within working condition, thus eliminating the need for using unnecessary heat actions. The designed DP algorithm and related results presented in this thesis does not indicate that it is possible to solely initiate preventive control actions before the coasting section. Further work to analyse this exposition is therefore suggested.

For a professional automotive engineer reading this thesis, the presented consumption results may seem to be unreasonably low. For the example of fuel consumption, the 13 litre EURO VI Scania engines which are in production are documented to have to have a fuel consumption within 205 and 210 g/kWh for the WHTC test cycle. In chapter 3.5.3 it was determined that the Simulink model underestimates approximately 3% compared to real measurements of the fuel consumption. This deviation factor is not included the results reported in this chapter. Taking the averaged simulated value of 198 g/kWh, compensating with 3% would give $198 \cdot 1.03 \approx 204$ g/kWh, which is closer to what the documented numbers indicate. However, the stated difference numbers are the same regardless of this compensation factor.

6

Conclusions and Future Work

6.1 Conclusions

The main objective of this thesis has been to examine the potential for improvement regarding the fuel consumption and keeping NO_x emissions within legal levels, when using a look-ahead control strategy. Due to difficulties of defining the factor of what NO_x emission level that is within legal limits, this project has focused on lowering both the consumed fuel and NO_x emission and comparing it to simulation results of today's performance. A temperature model for the aftertreatment system has been developed in Simulink which is used with simplified control system to establish estimations of today's performance. The method of determining an optimal control strategy has been made with the use of Dynamic Programming.

The results of the Dynamic Programming optimization indicates that preventive look-ahead control actions can be made to lower both the consumed fuel and emitted NO_x , compared to simulations of the system performance in present day. The results indicate that utilizing a more aggressive approach of lowering the control signal to lower modes in various sections, fuel consumption savings can be made. The amount of fuel and NO_x emissions that can be lowered is varied depending on the chosen parameter value of the weight constant β . The best case scenario of reducing fuel consumption is determined with $\beta = 0.06$, and with the Simulink model it is shown that the fuel consumption and NO_x emissions are lowered to 0.14% and 5.2% respectively.

6.2 Future work

The suggested future work can be divided into two categories, modelling and Dynamic Programming.

6.2.1 Modelling

For the used temperature models, which are presented in chapter 3, it was concluded that the model for $T_{DOC,in}$ is the deficient model for modelling the aftertreatment system more accurately. The subsequent models located after $T_{DOC,in}$, is determined to be good models of predicting temperatures accurately. Establishing a better non-linear model for $T_{DOC,in}$ to accurately predict temperatures for all types of driving patterns would therefore make the complete model more reliable.

6.2.2 Dynamic Programming

The main drawback with the DP algorithm used in this thesis is the implementation of the NO_x constraint. Investigating if it is possible to implement a more detailed NO_x constraint in closer relation to vehicle certification procedures, is of high interest. It may also be of interest to extend the DP-model with additional states to achieve a more accurate temperature model.

If a more detailed NO_x constraint is established which guarantees solutions within regulated levels, one could also change the objective function to take into account the costs of fuel and Adblue. An objective functions which minimizes the total cost of consumed fuel and Adblue would be of interest for companies who uses HDVs.

Another interesting feature to examine is to extend the DP algorithm to a *Boundary-Surface Dynamic Programming* algorithm, as described in [7]. The author of [7] encountered similar problems with incorrect results when the optimization evaluates infeasible points outside the gridded state space. By using Boundary-Surface Dynamic Programming the author achieves feasible solutions with a slight increase of optimization time.

Bibliography

- [1] Regulations Commission: "Regulation (EU) No 582/2011 of 25 May 2011 implementing and amending Regulation (EC) No 595/2009 of the European Parliament and of the Council with respect to emissions from heavy duty vehicles (Euro VI) and amending Annexes I and III to Directive 2007/46/EC of the European Parliament and of the Council," 2011. Cited on pages 1 and 2.
- [2] Alkemade, Ulrich G., and Bernd Schumann. "Engines and exhaust after treatment systems for future automotive applications," *Solid State Ionics* 177.26 (2006): 2291-2296. Cited on page 9.
- [3] Hellström, Erik. "Look-ahead control of heavy vehicles," PhD thesis, 2010, No. 1315, Linköping University. Cited on pages 2, 4, 33, and 43.
- [4] Hellström, Erik, et al. "Look-ahead control for heavy trucks to minimize trip time and fuel consumption," *Control Engineering Practice* 17.2 (2009): 245-254. Cited on page 4.
- [5] Gustafsson, Niklas. "The use of positioning systems for look-ahead control in vehicles," Master's thesis, 2006. LiTH-ISY-EX-06/3776-SE, Linköping University. Cited on page 5.
- [6] Hebbale, Kumaraswamy V., et al. "Using GPS/map/traffic info to control performance of aftertreatment (AT) devices," U.S. Patent No. 8,392,091. 5 Mar. 2013. Cited on page 5.
- [7] van Schijndel, J., et al. "Dynamic Programming for Integrated Emission Management in Diesel Engines." The International Federation of Automatic Control, Cape Town, South Africa. August 24-29, 2014. Cited on pages 5 and 58.
- [8] Birkhold, Felix, et al. "Analysis of the injection of urea-water-solution for automotive SCR DeNOx-systems: modeling of two-phase flow and spray/wall-interaction," No. 2006-01-0643. SAE Technical Paper, 2006. Cited on pages 9 and 10.

- [9] Chen, Pingen, and Junmin Wang. "Control-oriented model for integrated diesel engine and aftertreatment systems thermal management," *Control Engineering Practice* 22 (2014): 81-93. Cited on pages 5, 18, and 20.
- [10] Balaji, Mohan, et al. "Fuel injection strategies for performance improvement and emissions reduction in compression ignition engines – A review," Department of Mechanical Engineering, National University of Singapore, Cited on page 8.
- [11] Johansson, Bengt, "Förbränningsmotorer del 1," Avdelningen för Förbränningsmotorer, Lunds tekniska högskola, 2003. Cited on pages 7 and 8.
- [12] Söderstedt, Fredrik. "Fuel Consumption Estimation for Vehicle Configuration Optimization," Master's thesis, 2014. LiTH-ISY-EX-14/4775-SE, Linköping University. Cited on page 21.
- [13] Eriksson, Lars, and Nielsen, Lars. "Modelling and Control of Engines and Drivelines," John Wiley and Sons, 2014. Cited on pages 5, 7, 8, and 10.
- [14] Konstantinidis, P. A., et al. "Transient heat transfer modelling in automotive exhaust systems," Proceedings of the Institution of Mechanical Engineers, Part C: Journal of Mechanical Engineering Science 211.1 (1997): 1-15. Cited on page 5.
- [15] United Nations, "Proposal for the 06 series of amendments to UN Regulation No. 49 (Emissions of C.I. and P.I. (LPG and CNG) engines)," World Forum for Harmonization of Vehicle Regulations, 157th session, Geneva, 26-29 June 2012 Cited on page 10.
- [16] Kang, Jun-Mo, Ilya Kolmanovsky, and J. W. Grizzle. "Approximate dynamic programming solutions for lean burn engine aftertreatment," *Decision and Control*, 1999. Proceedings of the 38th IEEE Conference on. Vol. 2. IEEE, 1999. Cited on page 4.
- [17] Guzzella, Lino and Sciarretta, Antonio, "Vehicle Propulsion Systems", Springer, 2013 Cited on page 42.



Upphovsrätt

Detta dokument hålls tillgängligt på Internet — eller dess framtida ersättare — under 25 år från publiceringsdatum under förutsättning att inga extraordinära omständigheter uppstår.

Tillgång till dokumentet innebär tillstånd för var och en att läsa, ladda ner, skriva ut enstaka kopior för enskilt bruk och att använda det oförändrat för icke-kommersiell forskning och för undervisning. Överföring av upphovsrätten vid en senare tidpunkt kan inte upphäva detta tillstånd. All annan användning av dokumentet kräver upphovsmannens medgivande. För att garantera äktheten, säkerheten och tillgängligheten finns det lösningar av teknisk och administrativ art.

Upphovsmannens ideella rätt innefattar rätt att bli nämnd som upphovsman i den omfattning som god sed kräver vid användning av dokumentet på ovan beskrivna sätt samt skydd mot att dokumentet ändras eller presenteras i sådan form eller i sådant sammanhang som är kränkande för upphovsmannens litterära eller konstnärliga anseende eller egenart.

För ytterligare information om Linköping University Electronic Press se förlagets hemsida <http://www.ep.liu.se/>

Copyright

The publishers will keep this document online on the Internet — or its possible replacement — for a period of 25 years from the date of publication barring exceptional circumstances.

The online availability of the document implies a permanent permission for anyone to read, to download, to print out single copies for his/her own use and to use it unchanged for any non-commercial research and educational purpose. Subsequent transfers of copyright cannot revoke this permission. All other uses of the document are conditional on the consent of the copyright owner. The publisher has taken technical and administrative measures to assure authenticity, security and accessibility.

According to intellectual property law the author has the right to be mentioned when his/her work is accessed as described above and to be protected against infringement.

For additional information about the Linköping University Electronic Press and its procedures for publication and for assurance of document integrity, please refer to its www home page: <http://www.ep.liu.se/>